



1 **Grazing related nitrous oxide emissions: from patch scale to field** 2 **scale**

3 Karl Voglmeier^{1,2}, Johan Six², Markus Jocher¹, Christof Ammann¹

4 ¹Climate and Agriculture Group, Agroscope, Zürich, 8046, Switzerland

5 ²Department of Environmental Systems Science, ETH Zurich, Zürich, 8092, Switzerland

6

7 *Correspondence to:* Karl Voglmeier (karl.voglmeier@agroscope.admin.ch)

8 **Abstract.**

9 Grazed pastures are strong sources of the greenhouse gas nitrous oxide (N₂O). The quantification of the emissions is
10 challenging due to the strong spatial and temporal variability of the emission sources and therefore emission estimates are
11 very uncertain. This study presents N₂O emission measurements of two grazing systems in western Switzerland over the
12 grazing season 2016. Two herds of dairy cows were kept in an intensive rotational grazing management. The diet for the
13 cows consisted of different protein to energy ratios resulting in different N excretion rates. The N in the excretion was
14 estimated by an animal budget model taking into account the measurements of feed intake, milk yield and body weight of the
15 cow herds. Excreta patches and background surfaces on the pasture were identified manually after different grazing rotations
16 and the magnitude and temporal pattern of the single emission sources were measured with a Fast-box (FB) chamber. The
17 field scale fluxes were quantified using two eddy covariance (EC) systems. The FB measurements were finally up-scaled to
18 the field and compared to the EC measurements for quality control by using EC footprint estimates of a backward
19 Lagrangian stochastic dispersion model. Neglecting emission periods influenced by fertilizer applications resulted in
20 significant higher system emissions (960 ± 219 g N₂O-N, or 25 %) for the full grazing regime (system G) compared to the
21 system with the N balanced diet (system M). Relating the found emissions to the excreta N resulted in grazing related EFs of
22 1.24 ± 0.20 % for system M and 1.36 ± 0.26 % for system G. The found grazing related EFs were thus significantly smaller
23 compared to the EF of 2 % of the IPCC guidelines. Disaggregating the up-scaled fluxes into single contributors showed that
24 urine patch emission dominated the field scale fluxes (57 %), followed by significant background emissions (38 %) and only
25 a small contribution of dung patch emission (5 %). The resulting EFs of 1.13 ± 0.3 % and 0.17 ± 0.04 % for urine and dung
26 indicates the need to disaggregate the grazing related EFs by excreta type. The study also highlights the advantage of an N
27 optimised diet which resulted in reduced N₂O emissions on the system level.

28 **1 INTRODUCTION**

29 In the atmosphere, nitrous oxide (N₂O) is a strong greenhouse gas (GHG) with a 298 times stronger warming potential
30 compared to CO₂ on a mass basis. Typically an inert gas in the troposphere, it has a strong potential to destroy the ozone
31 layer in the stratosphere (Portmann et al., 2012). The largest share of N₂O emissions are attributed to fertilization in the



1 agricultural sector but also livestock grazing, especially by cows, can lead to significant direct and indirect N₂O emissions
2 due to excreta from the animals (Luo et al., 2017; Reay et al., 2012). Averaged over many climatic conditions and farms, the
3 nitrogen (N) deposited by the excreta of animals often even exceeds the N applied by fertilizer (Aarons et al., 2017). Directly
4 applied on a pasture soil, microbial nitrification and denitrification processes transform the reactive nitrogen of excreta and
5 significant amounts of N₂O can be produced as a by-product (Selbie et al., 2015). A non-linear response of N₂O emissions to
6 N loading was shown previously (Cardenas et al., 2010) and urine patches of cattle have exceptionally high loading rates (up
7 to 2000 kg N ha⁻¹) making them especially prone to high N₂O losses (Selbie et al., 2015).

8 For inventories and live cycle assessments, the magnitude of the emissions is usually calculated by applying a bulk emission
9 factor (EF) to the estimated N excretion by animals. Countries often use the default Tier 1 EF of 2% for grazed pastures
10 according to the guidelines of the Intergovernmental Panel on Climate Change (IPCC, 2006). However, the default Tier 1
11 approach regularly overestimates the emissions (Bell et al., 2015; Chadwick et al., 2018a) and the default EF does not take
12 country specific conditions (climate, soil, management) into account. Therefore, many countries have already developed a
13 country specific EF (Tier 2, e.g. New Zealand, Saggar et al., 2015) which is still lacking for Switzerland. Additionally, it has
14 been shown that an excreta specific EF for urine and dung might be beneficial in describing the emissions and understanding
15 the contributions of the different emission sources on a pasture (Bell et al., 2015). A better understanding of the individual
16 contributions would also be very helpful to reduce the emissions. However, reported uncertainties of excreta specific EFs are
17 rather high (e.g. EF of 0-14% of applied urine N, n=40; Selbie et al., 2015) and many of those studies measured the
18 emissions on artificially applied urine or under laboratory conditions and thus these results are questionable with regard to
19 the applicability within greenhouse gas inventories.

20 The more efficient use of N is essential to reduce these emissions. Studies have shown (e.g. Arriaga et al., 2010) that an
21 optimised feeding strategy can lead to less N excreted by the animals. For this purpose forage with a low N content (e.g.
22 maize) can be fed as a supplement to N rich grass and this subsequently leads to less N in the excreta, mainly in form of less
23 urine N. A lower amount of N input to the pasture is supposed to produce less N₂O emissions but emission experiments
24 under real practice conditions for a full grazing season are very rare.

25 Historically, most studies used static chambers to quantify N₂O emissions (Flecharde et al., 2007). Chamber measurements
26 are ideal to quantify emissions on a small scale and to attribute them to certain emission drivers, but for excreta emissions
27 these measurements were often performed on manually applied urine and dung patches (Bell et al., 2015; Cai and Akiyama,
28 2016). Additionally, due to the strong heterogeneity of the emissions from a pasture (Cowan et al., 2015; Flecharde et al.,
29 2007) chamber techniques are not ideal to compute field scale emissions for grazing systems. The eddy covariance (EC)
30 method overcomes this problem by integration over a larger domain. It was already applied successfully to quantify N₂O
31 emissions from pastures and grasslands (Jones et al., 2011). Some studies also tried to compare different systems (intensive –
32 extensive, different crops, land / lake, ...) with one EC tower (e.g. Biermann et al., 2014; Fuchs et al., 2018) by partitioning
33 the fluxes based on wind direction and systems geometry, but typically one tower for one system is preferable. In order to
34 understand and quantify the emissions of a pasture, the combined approach of EC measurements and chambers is regarded



1 as the best solution (Cowan et al., 2015). The EC systems can be used to quantify the field scale emissions while the
2 chamber approach can be used to understand the contributions of the single emission sources (urine patches, dung patches
3 and other "background" areas).

4 In our experiment, we measured N₂O emissions of two neighbouring pastures simultaneously with the EC method over a full
5 grazing season. The two pastures differed in the energy to protein balance of the diet for the cows. The small scale fluxes
6 were quantified with a Fast box chamber and up-scaled to match the EC flux footprints for comparison. Further on, we
7 computed the contribution of the different emission sources to the overall pasture emissions. The results were compared to
8 values provided by IPCC and other literature values. We aimed at a better understanding of the quantity of the overall
9 pasture emissions, the different emission sources and the reduction of corresponding uncertainties.

10 **2 MATERIAL AND METHODS**

11 **2.1 Experimental site**

12 The experiment was conducted at the research farm Agroscope Posieux in the Pre-Alps of Switzerland in the canton of
13 Fribourg (46°46'04"N, 7°06'28"E) and has been already described in detail in Voglmeier et al. (2018). The farm is located
14 at an elevation of 642 m with an annual average temperature of 8.7 °C and an annual average rain amount of 1075 mm
15 (MeteoSwiss, 2018). The soil consisted mainly of a stagnic Anthrosol with a loamy texture (about 20 % clay, 35 % silt and
16 45 % sand, see Table 1). Soil measurements were performed at different depth and four locations on the pasture in 2013 and
17 2016. The vegetation consists of a grass-clover mixture typical for Swiss pastures (10 % to 50 % *Lolium perenne* and 7 % to
18 40 % *Trifolium repens*). After the last renovation of the field in 2007 the field was used as an intensive pasture for cattle with
19 occasional grass cuts for maintaining a homogenous sward. Beside the excreta from the animals, the fertilization rate was in
20 the order of 120 kg N ha⁻¹ per year between 2007 and 2015.

21 **2.2 Experimental design**

22 The experiment took place at a 5.5 ha pasture, which was divided into two separate systems differing in feeding strategy of
23 the 12 cows per system. The northern system (system M) represented a N optimized feeding option where the diet of the
24 cows consisted of grass with additional maize silage (roughly 20 % of the dry matter intake (DMI)) resulting in a demand
25 optimized protein content in the diet (Arriaga et al., 2010; Yan et al., 2006). This also reduced the N input to the pasture. The
26 southern system (system G) represented a full grazing regime with no additional forage which resulted in a considerable
27 protein surplus. Both systems were managed as a rotational grazing system with 11 paddocks (Fig. 1a) resulting in a typical
28 rotation period of about 20 days. The size of the paddocks was adjusted for the different feeding strategies and resulted in
29 typical sizes of 1700 m² for system M and 2200 m² for system G. The rotation of both systems was managed synchronously
30 with a new rotation starting on the westerly paddocks (X.11 to X.16 with X indicating both systems) followed by the easterly
31 ones (X.21 to X.25).



1
2 Grazing on the paddocks started with intermittent grazing phases in March and ended in early November with the main
3 grazing season being between end of April and early October. During this time period eight full rotations took place. The
4 cows typically spent 18 to 20 hours per day on the pasture and were brought to the barn twice a day (around 05:00 and 17:00
5 LT) for milking. However, in July and August the cows spent a longer time in the barn during daytime (up to six hours, see
6 Fig. 2c) mainly due to high air temperatures and to a minor degree due to additional experiments of other research groups.
7 Heavy rain events in June led to very wet soil conditions which prevented grazing between the 8th of June and 4th of July and
8 made a grass cut on the 22nd of June necessary.

9 **2.3 N input to the pasture**

10 During the grazing season, N input to the pasture mainly occurred in the form of excreta of the grazing animals and to a
11 lesser extent as mineral fertilizer (Fig. 2d). The mineral fertilizer was ammonium nitrate (28 kg ha⁻¹) applied at the end of
12 June and urea (42 kg ha⁻¹) with a split application between mid of August (western paddocks X.11–X.16) and early
13 September (eastern paddocks X.21–X.25) due to concurrent grazing. For this study the N input by grazing excreta was
14 particularly important in order to compute the grazing related EF and to compare the results of this study with literature
15 reports and emission inventory models. For the comparison with the field-scale EC method the N excretion was also needed
16 to estimate the number of dung and urine patches which were subsequently needed to upscale the small scale chamber
17 measurements to the field scale (Sect. 2.7). Because N excretion cannot easily be measured in the field, we estimated it with
18 a Swiss dairy cow nitrogen budget model. In short, this model balances the N flows in the cow by using measured
19 daily/seasonal N in the feed input, storage in body weight gain and milk to give an output of daily values of urine and dung
20 N. For further details see explanation in Voglmeier et al. (2018) who also estimated the corresponding uncertainty of the
21 total N and urine / dung N to be 15 % (2 σ) for the same experiment. Seasonal statistics of the input variables are given in
22 Table 2.

23 **2.4 Small scale flux measurements**

24 **2.4.1 Excreta detection**

25 The localisation of fresh dung and urine patches was essential in this study to perform chamber measurements attributable to
26 distinct surface conditions. Intensive observation areas of 10 x 10 m or 15 x 15 m close to both EC towers in the paddocks
27 X.11 and X.21 (see Fig. 1a) were selected. Within these areas fresh dung and urine patches were mapped typically 1-3 days
28 after grazing of the respective paddock. Dung pats were mapped visually and labelled for subsequent chamber
29 measurements. For urine patches a direct visual identification was not possible. Bates et al. (2015) demonstrated the ability
30 of surface-soil electrical conductivity measurements to detect urine patches. Using this approach we mounted a GS3 probe
31 (Meter Group, US; for soil moisture, temperature and electrical conductivity measurements) on a hand-held stick and



1 mapped the intensive observation area on a 25 cm grid (Fig. 3). Conductivity values exceeding a threshold of 0.15 mS cm^{-1}
2 were marked as possible urine patches for further chamber measurements. Chamber measurements on areas not affected by
3 urine patches (blue areas in Fig. 3a) were considered as ‘background’ fluxes without recent influence of excreta. Exemplary
4 continuous electrical conductivity measurements (Fig. 3b) on manually applied urine patches in 2017 illustrate the long term
5 effect and demonstrated the possibility to distinguish between background areas and urine patches more than 10 days after
6 the application of urine.

7 **2.4.2 Fast-box measurements**

8 Small scale emissions from urine and dung patches as well as background pasture areas were measured with the fast-box
9 (FB) chamber (Hensen et al., 2006). The measurements took place on the paddocks X.11 and X.21 (Fig. 1a) between
10 beginning of July and mid of October and were therefore taken mainly during dry soil conditions (Fig. 2). Measurements
11 usually started after the excretion detection (Sect. 2.4.1) and about 1-2 days after end of grazing (EOG). The age of the
12 excreta patches is important for the interpretation of the measured fluxes. However, the exact determination of the excreta
13 age was not possible. Thus, the time since EOG was used as excreta age for each FB measurement. The potential age
14 variability of a single excreta patch resulted from the sojourn time of the cows on the paddock which typically was in the
15 range of 1–1.5 days.

16 The manually-operated opaque $0.8 \text{ m} \times 0.8 \text{ m} \times 0.5 \text{ m}$ box was connected to a fast response quantum cascade laser analyser
17 (QCL, Aerodyne Research Inc.) that was also used for the EC system on the respective field (see below Sect. 2.5.1). The gas
18 was sucked through a $40 \text{ m } 1/4''$ PA tube allowing measurements within a radius of about 35 m on the paddocks X.11 and
19 X.21 (see Fig. 1). The sample flow rate Q was typically around 8 l min^{-1} . The box was modified by using a defined air inlet
20 through a 4 cm hole on top of the box, which was connected to a 1 m tube. The inlet of the tube was packed with a 10 cm
21 foam material to avoid uncontrolled air exchange due to wind induced pressure fluctuations outside the chamber. The
22 chamber was also equipped with a GMP343 (Vaisala, FL) CO_2 probe to measure the soil respiration. The increase in
23 concentration after placing the chamber on the soil was recorded every three seconds for a time period of about 90 seconds.
24 The inflow of background concentration C_{bg} into the chamber through the inlet lead to lower measured concentration values
25 C . This can be described by the following differential equation for the chamber headspace concentration $C(t)$:

$$V \frac{\delta C}{\delta t} = A \cdot F_{\text{Cham}} - Q(C - C_{\text{bg}}) \quad (1a)$$

27

28 This is a combination of the two equations for static chambers (left-hand term = 0) and for the dynamic chamber (rightmost
29 term = 0). Solving of the equation yields the explicit time function:

30



$$C(t) = \frac{A \cdot F_{\text{Cham}}}{Q} \left(1 - e^{-\frac{Q}{V}t}\right) + C_{\text{bg}} \quad (1b)$$

1
2 For small values of the exponent $Q/V \cdot t$ (slow chamber volume exchange and short measurement time) as characteristic for
3 the present fast-box measurements, the entire bracket term can be linearized with a series expansion to $(Q/V \cdot t)$. Inserting the
4 resulting function for $C(t)$ into Eq. 1a yields:

$$V \frac{\delta C}{\delta t} = A \cdot F_{\text{Cham}} \left(1 + \frac{Q}{V}t\right) \quad (1c)$$

6
7 With the FB dimensions and sampling flow rate as given above and a maximum accumulation time $t \leq 2$ min, the deviation
8 from the ideal linear increase of a fully closed static chamber was $\leq 5\%$. The flux was finally calculated by using the HMR
9 package (Pedersen et al., 2010) which uses linear and non-linear regression to fit the measured concentration values. The
10 uncertainty of an individual box measurement is estimated to be around 20 % (Hensen et al., 2006).

11 In order to relate the measured fluxes to environmental driving parameters the following sensors were placed inside on the
12 chamber: a thermocouple for air temperature measurement within the chamber, a GS3 probe (see Sect. 2.4.1) and a ML3
13 Thetaprobe (Delta-T Devices Ltd, UK) for soil moisture and temperature observations (c. 0-5 cm and 0-10cm depth,
14 respectively). All measured data values were stored on a data logger mounted on top of the box and transferred to a computer
15 in the nearby shelter or trailer. A customized LabView (National Instruments, US) program allowed for online inspection of
16 all measured data values including the gas concentrations.

17 2.4.3 Quality control and system comparison

18 FB fluxes were selected for post-processing after fulfilling certain quality criteria. In a first step, the R-squared value of any
19 flux calculation had to exceed 0.9 (e.g. for N_2O flux either the R-squared value of N_2O , CH_4 or CO_2 had to exceed 0.9). For
20 urine patches, the soil conductivity had to exceed 0.25 mS cm^{-1} at the beginning of the measurements (see also Fig. 3b)
21 because sometimes possible old urine patches (of previous management rotations) were observed. Presumable old patches
22 were therefore rejected for further processing. Background fluxes were removed from further processing if the flux value
23 exceeded $40 \mu\text{g m}^{-2} \text{ h}^{-1}$ ($=4 \times$ median value) to ensure that undetected urine patches at the chamber surroundings did not
24 influence the flux measurements. Finally, 360 and 293 flux measurements met the criteria on system M and G, respectively.
25 These measurements were composed of 238 background fluxes, 242 urine patch fluxes and 173 dung fluxes.
26 The two pasture systems were compared by ordering the fluxes based on their magnitude on a given day for each system and
27 source class. Due to the synchronous grazing regime, the fluxes represent the same excreta age (e.g. on day 3 after EOG).
28 However, synchronous FB measurements on both systems were not always performed. Resulting numbers of data pairs are
29 46, 54 and 40 for background, urine and dung fluxes, respectively.



1 2.5 Field scale flux measurements

2 2.5.1 Eddy covariance system

3 For field scale flux measurements EC towers were installed in the middle of the two pasture fields to account for the
4 predominant wind directions north-east and south-west (Fig. 1) and were fenced to avoid unwanted animal contact. The
5 measurement height was 2 m which enabled a good footprint coverage (Fig. 4, Sect. 2.5.4) of both fields and allowed to
6 measure fields-scale fluxes of both systems.

7 The two EC systems were identically equipped with an ultra-sonic anemometer-thermometer (further on named sonic, HS-
8 50, Gill Instruments Ltd., UK) to quantify the turbulent mixing by measuring the three dimensional wind velocity (u,v,w)
9 and air temperature. Dry air mixing ratios of N₂O were measured with closed-path quantum cascade laser spectrometers
10 (QCL, QC-TILDAS, Aerodyne Research Inc.) that analysed air samples sucked through a 25 m PA tube (inner diameter 6
11 mm) by a vacuum pump (Bluffton Motor Works, flow rate ca. 13 l min⁻¹). One filter at the inlet (AcroPak, Pall Corporation)
12 and one before the instrument (Midisart 2000, Sartorius Stedim Biotech GmbH) were used for each system to filter out
13 particles. The inlets of the QCLs were separated from the centre of the sonic head by around 20 cm and the QCL instruments
14 were placed in a temperature controlled environment (trailer at system M, shelter at system G) some 20 meters north (system
15 M) or south (system G) of the EC towers.

16 The sample frequency of the EC system was generally 10 Hz. A customized LabView (National Instruments, US) program
17 was used to combine the data strings of the individual instruments and store them as binary raw data for offline analyses.
18 Additionally the program visualized the measurements and fluxes of an online flux calculation and allowed to check the EC
19 system by remote access.

20 2.5.2 Flux calculation

21 A customized program written in the statistical software R (R Core Team, 2016) was used to calculate EC fluxes for 30 min
22 intervals (similar to Felber, 2015a; Felber et al., 2015b). The approach is based on Ammann et al. (2006, 2007). In a first
23 step, 10 Hz data outside a plausible physical range were identified and replaced by a running mean filter with a window size
24 of 500. In a next step, wind compounds were rotated into the mean wind direction using the double rotation (Kaimal and
25 Finnigan, 1994) technique and concentration values were subject to linear detrending within an averaging interval of 5 min.

26 The EC flux is defined as the covariance of the vertical wind speed and the trace gas mixing ratio. Due to the long inlet tube
27 the time series of the trace gas signals are delayed in relation to the wind measurements (by a quasi-constant lag time of
28 several seconds) and have to be shifted to obtain the correct covariance flux (Langford et al., 2015). In a pre-evaluation, the
29 'default lag' was determined as the most frequent position of the maximum absolute value of the cross-covariance function
30 over periods of weeks to months (depending on instrument maintenance). Then it was checked for each half-hour period
31 whether the individual 'dynamic' lag was within a time window of 0.61 seconds around the default lag. If this was the case,



1 the dynamic lag was used, otherwise the default lag. In order to minimize the effect of non-stationarities in the time series,
2 the 30 min flux was finally calculated as average over six 5 min subinterval flux values.
3 The fluxes measured by EC systems are subject to different high frequency losses due to sensor separation and in case of
4 N₂O air transport through the inlet tubes (Foken et al., 2012). These damping effects can lead to significant underestimation
5 of the flux and must be corrected. Based on Ammann et al. (2006) the half-hourly high frequency losses were quantified
6 using the ‘ogive’ method where the damping factor was calculated by fitting the normalized cumulative co-spectrum of N₂O
7 to the one of the sensible heat at a frequency of 0.065 Hz. In a post processing step, these half-hourly damping factors were
8 filtered for favourable conditions e.g. low noise level of the ogive and the flux. The selected values were used to compute a
9 wind speed and stability dependent damping function which was finally used to estimate the damping factor. Depending
10 mainly on the wind speed, a damping effect of 10 – 30 % was found and corrected for.
11 EC flux measurements were taken continuously over the grazing season. Since the present study is focussed on N₂O
12 emissions from grazing, time periods with strong influence of N₂O emissions from fertilization and harvest events (see Fig.
13 2) were excluded for computation of cumulative emissions and for comparisons between field scale and small scale
14 measurements. These exclusion periods were limited to the 15 d following fertilization or harvest and led to a rejection of 47
15 days during the grazing season. The criterion is based on observed EC fluxes (Sect. 3.1) and is in accordance with Jones et
16 al. (2011). The time periods used for calculation of the cumulative grazing emissions are further on defined as grazing-only
17 periods (GOP) and accumulated to 198 days.

18 **2.5.3 Quality control and gap filling**

19 EC flux measurements are subject to different sources of measurement problems and quality issues which often result in data
20 loss or necessitate data rejection. These sources can be instrument specific like power failures or malfunctioning,
21 environmental driven like measurements under non ideal conditions (e.g. low turbulence) or a combination of both (Papale,
22 2012). Power break down, instrument maintenance (only on system M) and delayed installation (only on system G) led to a
23 data loss during the GOP of 12 and 17 % for systems M and G, respectively. Data rejection due to low u_* ($<0.07 \text{ m s}^{-1}$), non-
24 stationarity (Foken et al., 2012) and large vertical tilt angle ($-2^\circ - 6^\circ$) of the wind vector led to a further data loss of about 35
25 %. Additional rejection of wind sectors influenced by the farm facilities, trailer or shelter and to avoid cross-influences from
26 the other pasture system ($280^\circ - 25^\circ$; $97^\circ - 195^\circ$) contributed to an overall data loss of 64 and 69 % for systems M and G.
27 The data gaps had a diurnal pattern with stronger data loss during the night. It was driven by the wind pattern with typically
28 stronger wind speeds during daytime and calm nights.
29 The gaps in the flux time series needed to be filled in order to compute cumulative sums over a certain period of time.
30 However, no well-established reference method for the gap filling of N₂O fluxes exists to date. We followed the evaluation
31 of Mishurov and Kiely (2011) and used a lookup table method (LUT) with three parameters: one for the preceding
32 cumulative rainfall of the last 12 hours with three classes (no rainfall, 0-2 mm, >2 mm), one for the percentiles of the soil
33 temperature at 5 cm depth with four classes (0-25th percentile, >25 th percentile – median, $>$ median – 75th percentile, >75 th



1 percentile), and one for the footprint-weighted (Sect. 2.5.4) averaged cow density (cows ha⁻¹) on the single paddocks over
2 the preceding five days (0, 0 – 2, > 2 cows ha⁻¹). To check the sensitivity towards different gap filling methods three other
3 techniques were compared to the LUT approach. [I] Running mean with a variable filter window size and at least 12 values;
4 [II] Monthly mean diurnal variation (MDV, see Zhao and Huang, 2015) with a running half hourly window size of five in
5 order to have more values during night-time, [III] seasonal MDV based on half-hourly values averaged over the whole
6 grazing season. The uncertainty of gap filling for seasonal cumulative fluxes was estimated from the standard deviations of
7 monthly cumulative fluxes retrieved with the different gap filling methods during GOP. It resulted in an uncertainty of 14
8 and 18 % for the system M and G, respectively (1 σ). It was assumed, that this uncertainty reflects the sum of all important
9 individual uncertainties of the cumulative emissions (e.g. Sect. 3.3.1 and 4). Due to the delayed installation of the EC tower
10 on the southern field all values prior to the 14th of April on system G resulted from the gap filling routine.

11 2.5.4 Footprint modelling

12 EC measurements yield a spatially integrated flux over a certain area represented by the flux footprint (Schmid, 2002). In the
13 present study, this footprint typically extends over multiple grazing paddocks depending on wind direction and turbulence
14 intensity. Therefore quantitative footprint information is needed for the comparison of the EC fluxes with the up-scaled FB
15 measurements (Sect. 2.7), and it has to be checked for the spatial dimension to be sure that the measured flux is mainly
16 dominated by the area of the system and not contaminated by the neighbouring systems (either the other system or fluxes
17 originating from surrounding fields). In this study an open source version of a backward Lagrangian Stochastic dispersion
18 footprint model was used (Häni, 2017; Häni et al., 2018). It is based on Flesch et al. (2004) and the flux to emission ratio is
19 calculated following Eq. 2 with F being the measured EC flux, E the emission strength of the source, N the number of
20 released particles, n_t the number of touchdowns within the source, w_{ini}^i the release and w_o^i the touchdown velocity of the
21 particle.

$$\frac{F}{E} = \frac{2}{N} \sum_{i=1}^{n_t} \frac{w_{ini}^i}{w_o^i} \quad (2)$$

22 In order to calculate the footprint, 80'000 trajectories were released backwards in time using the wind and turbulence
23 parameters calculated from the sonic measurements of the EC systems. The individual flux contributions from the paddocks
24 were calculated from the provided geometric information of the source areas (paddocks). The systematic uncertainty of the
25 bLS model was estimated to be in the range of 10 % (Flesch and Wilson, 2005; Wilson et al., 2013).

26 The integral footprint extension, taking into account the wind direction and u_* filtering as described in Sect. 2.5.3, resulted in
27 a distinct separation of the two systems (Fig. 4) with only marginal contributions of the other system (<2.5 %). The seasonal
28 averaged footprint ratios during the grazing season covered about 80 % of the main field (without the optional areas
29 indicated in grey colour in Fig. 1a). The footprint ratios of the single paddocks were also used to upscale small scale
30 emissions to the EC flux footprint in order to compare the two flux measurement methods to each other.



1 **2.6 Environmental parameters**

2 In order to relate the measured fluxes to meteorological driving parameters an automated weather station (Campbell Scientific
3 Ltd., UK) was installed at the northern field next to the Sonic. A WXT520 (Vaisala, Vantaa, FL) measured the wind speed,
4 precipitation, temperature and barometric pressure, and global radiation was measured with a pyranometer (CNR1,
5 Kipp&Zonen, Delft, NL).

6 Soil moisture and temperature were measured continuously with two repetitions on each pasture system close to the EC
7 towers with ML3 Thetaprobe (Delta-T Devices Ltd, UK) devices at a depth of 5, 10, 20 and 40 cm.

8 **2.7 Upscaling of chamber measurements to eddy covariance footprint**

9 Pasture N₂O emissions result from a combination of ‘hotspot’ emissions from urine and dung patches and of ‘background’
10 emissions from the other pasture areas. Even though the FB measurements (Sect. 2.4.2) allowed for quantification of single
11 emissions sources, quantifying the contributions to the overall pasture emission is challenging due to the inherent
12 heterogeneous nature of these emissions (e.g. spatial dimension, emission strength, temporal behaviour, number of excreta
13 patches, ...). The EC method, on the other hand, allowed to measure the combination of all pasture sources by integrating
14 over multiple paddocks (see footprint, Fig. 4).

15 Upscaling FB measurements to the EC footprint was performed to allow a direct comparison between the two measurement
16 approaches and to compute the contribution of the different emission sources to the overall pasture emission. The upscaling
17 procedure is illustrated in Fig. 5. The number of urine and dung patches on the paddocks was estimated by using the daily N
18 excretion rate (Sect. 2.3), the daily grazing duration of the cows, a N loading of 22 g N per urination event (Misselbrook et
19 al., 2016) and of 12.5 g N per dung pad (Cardenas et al., 2016). During the grazing season, about 12.5 dung patches d⁻¹ cow⁻¹
20 and a number ratio of dung to urine patches of 1.3 for system M and 1.1 for system G was calculated. This compares well to
21 values from literature (Orr et al., 2012; Oudshoorn et al., 2008; Villettaz Robichaud et al., 2011). Due to very similar field
22 scale N₂O emission pattern (Sect. 3.1) and comparable soil measurements (Fig. 2), it was assumed that soil parameters were
23 homogenous on the pasture and that the measurements on system M were representative for the whole field.

24

25 The FB derived N₂O emissions for the different sources were analysed for potential driving parameters (excreta age, soil
26 temperature, soil moisture). For this purpose various regression models were tested using different predefined function types
27 (linear, exponential, polynomial functions, sigmoidal). Based on goodness of fit and statistical significance of regression
28 coefficients, the most suitable relationships were chosen and applied to produce continuous emission time series for the
29 paddock areas (Fig. 5):

30

31 (I) Background fluxes were parametrized as a function of soil moisture at a depth of 5 cm using the soil profile information
32 provided in Sect. 2.4 by using a logistic regression.



1 (II) Urine patch emissions were parametrized as an exponential decay function of excreta age. To account for different
2 environmental conditions, the deviations of the single emissions to this temporal emission pattern was again parametrized as
3 a function of soil temperature and moisture at a depth of 5 cm (Sect. 2.6). Upscaling to the paddocks size involved additional
4 information on the computed number density of urine patches (as mentioned previously).

5 (III) Dung patch emissions were parametrized as a second order polynomial function of excreta age. Paddock emissions were
6 calculated by applying this function to the computed number of dung patches (as previously mentioned) per paddock.

7 The up-scaled paddock emissions were finally compared to the EC fluxes by applying the computed footprint ratios (Sect.
8 2.5.4) in order to quantify the uncertainty of the upscaling process. Furthermore, the contribution of the individual emission
9 sources was computed from the up-scaled field scale emissions of the single emission sources.

10 **3 Results**

11 **3.1 EC fluxes**

12 Observed EC fluxes on both pasture systems showed an almost identical temporal pattern (Fig. 6). They varied significantly
13 during the grazing season with clear peaks after fertilization (grey shaded areas) and after grazing phases in the nearby
14 paddocks (e.g. peaks in May, beginning of August). The overall highest emissions (28.7 and 21.6 g N₂O-N ha⁻¹ h⁻¹ for system
15 M and G) were measured directly after the fertilizer application, which followed a harvest of hay at the end of June. The
16 partial fertilizer application in mid of August resulted in higher fluxes compared to the following one in early September.
17 The relatively high emissions during the first full grazing event beginning of May were characterized by high soil moisture
18 contents (see also Fig. 2a) whereas the very wet soil conditions and the corresponding grazing break during June resulted in
19 low fluxes in both systems. The small observed fluxes from mid of March until end of April resulted mainly from
20 background fluxes and sporadic grazing (Fig. 2c). Occasional negative individual flux values were observed in both systems
21 with values down to -1.20 and -1.56 g N₂O-N ha⁻¹ h⁻¹ for system M and G, respectively. These negative values were typically
22 observed during wet soil conditions but varying soil temperatures. On average, N₂O uptake was observed in 8 % and 7 % of
23 all 30 min EC fluxes for system M and G.

24 During the GOP (excluding the grey shaded fertilizer influenced time periods in Fig. 6), the fluxes were still very similar for
25 the two pasture systems M and G with a mean and standard deviation of 0.32 ± 0.36 vs 0.33 ± 0.37 g N₂O-N ha⁻¹ h⁻¹,
26 respectively. A mean diurnal cycle of the measured fluxes could be observed in both systems with highest values typically
27 occurring in the afternoon and, on average, about 10 – 20 % lower values during the night.



1 3.2 Chamber fluxes

2 3.2.1 Comparison of pasture systems

3 Fluxes of background and dung patches were significantly smaller compared to the fluxes of urine patches (Table 3, Fig. 7).
 4 Especially fresh deposited urine patches with excreta ages below 3 days were able to emit more than 100 times the values of
 5 typical background areas. The relative variability within the different source classes were very high and resulted in standard
 6 deviations larger than the associated mean values. The excreta fluxes measured on system G tended to be somewhat higher
 7 in magnitude, but no significant difference ($p > 0.05$) due to the large variability was found. Also for the background fluxes no
 8 significant ($p > 0.05$) difference between the two pasture systems was observed. Therefore all FB fluxes were combined for
 9 further processing without taking into account the different pasture systems.

10 3.2.2 Dependence on excreta age

11 The information on the temporal pattern of the excreta and background fluxes after grazing is important for the time
 12 integration of the individual sources and for the comparison with the EC measurements. In order to analyse and parameterize
 13 the temporal evolution of the emissions, the FB fluxes of each source class (background, urine, dung) were related to the
 14 days after EOG (defined as excreta age, Sect. 2.4.2) Δt_{EOG} (Fig. 8). A strong relation between measured excreta fluxes and
 15 Δt_{EOG} was found. This was especially pronounced for urine patches. Highest average urine patch fluxes $F_{U,temp}$ were observed
 16 in the first 6 days after EOG with the highest average value found on day one ($660 \mu\text{g N}_2\text{O-N m}^{-2} \text{h}^{-1} \pm 983 \mu\text{g N}_2\text{O-N m}^{-2} \text{h}^{-1}$,
 17 mean \pm std). However, a large variability of the single fluxes was observed as well. The absolute highest $F_{U,temp}$ was
 18 retrieved on day 6 ($5117 \mu\text{g N}_2\text{O-N m}^{-2} \text{h}^{-1}$) but even after 15 days very high individual fluxes were observed (up to $2861 \mu\text{g}$
 19 $\text{N}_2\text{O-N m}^{-2} \text{h}^{-1}$). Mainly depending on environmental conditions (see Sect. 3.2.3) fluxes could vary by two orders of
 20 magnitudes for a similar excreta age. Dung patch emissions $F_{D,temp}$ showed a relation to excreta age, however less
 21 pronounced compared to urine patches, and the highest averaged fluxes were observed between 4 – 11 days after dung
 22 deposition. Within this time period, fluxes nevertheless had a considerable variability and daily averages ranged between 16
 23 – $71 \mu\text{g N}_2\text{O-N m}^{-2} \text{h}^{-1}$ and thus were significantly smaller compared to $F_{U,temp}$.

24 While excreta patch emissions showed a clear response to excreta age, background fluxes stayed rather constant with small
 25 values and no obvious temporal pattern and were significantly smaller compared to urine patch emissions. In order to
 26 parametrize $F_{U,temp}$ an exponential decrease (Fig. 8) was fitted to the averaged measured flux values within 3 days (Eq. 3).

27

$$28 \quad F_{U,temp} = a_1 \cdot \exp^{b_1 \cdot \Delta t_{EOG}} \quad (3)$$

29

30 The coefficients of Eq.3 – Eq.8 are presented in Table 4 and the resulting fluxes are calculated in units of $\text{g N}_2\text{O-N m}^{-2} \text{h}^{-1}$.
 31 $F_{D,temp}$ was parametrised with a second order polynomial regression (Eq. 4) to the available 3 daily averages and negative
 32 values were set to zero ($\approx \Delta t_{EOG} > 25 \text{ d}$).



1

$$F_{D,temp} = a_2 + b_2 \cdot \Delta t_{EOG} - c_2 \cdot \Delta t_{EOG}^2 \quad (4)$$

3

4 3.2.3 Dependence on environmental conditions

5 Measured chamber fluxes were analysed in relation to driving soil parameters (Sect. 2.6). For dung patch emissions, no
 6 relation to these parameters was found. For background fluxes no significant dependence on soil temperature was found
 7 ($p < 0.05$), but a clear dependence on the volumetric water content (VWC) at a depth of 5 cm. The background fluxes had a
 8 large variability and could roughly be separated by three different VWC sectors. In the sector below a VWC of 0.27, fluxes
 9 typically ranged between $-3 \mu\text{g N}_2\text{O-N m}^{-2} \text{ h}^{-1}$ and $15 \mu\text{g N}_2\text{O-N m}^{-2} \text{ h}^{-1}$ whereas in the upper sector above a VWC of 0.33 the
 10 fluxes showed typical values between $0 \mu\text{g N}_2\text{O-N m}^{-2} \text{ h}^{-1}$ and $30 \mu\text{g N}_2\text{O-N m}^{-2} \text{ h}^{-1}$. Nevertheless, the variability was
 11 especially pronounced in the VWC range between 0.27 and 0.33 with fluxes ranging between $0 \mu\text{g N}_2\text{O-N m}^{-2} \text{ h}^{-1}$ and $40 \mu\text{g}$
 12 $\text{N}_2\text{O-N m}^{-2} \text{ h}^{-1}$. Thus this VWC range also comprised of the overall highest background fluxes. However, averaging the
 13 fluxes by VWC intervals of 0.05 resulted in very comparable values of about $12 \mu\text{g N}_2\text{O-N m}^{-2} \text{ h}^{-1}$ above a VWC of 0.3.
 14 Hence, the measured background fluxes could be parametrised with the following functional relationship:

15

$$F_{BG} = \frac{a_3}{1 + \exp((b_3 - VWC)/c_3)} \quad (5)$$

17

18 This logistic regression curve has a strong effect below VWC values of 0.30 but stays fairly constant at higher VWC
 19 contents and converges to a flux of $12.6 \mu\text{g N}_2\text{O-N m}^{-2} \text{ h}^{-1}$. Below a VWC of 0.2 the logistic regression converges to a
 20 background flux of $0 \mu\text{g N}_2\text{O-N m}^{-2} \text{ h}^{-1}$.

21 Measured urine patch emissions not only showed a clear response to the excreta age as shown in Sect. 3.2.2 but also to
 22 changes in T_S and VWC . On a specific Δt_{EOG} , $F_{U,temp}$ could vary significantly and correlated typically with soil conditions. The
 23 highest flux ($5117 \mu\text{g N}_2\text{O-N m}^{-2} \text{ h}^{-1}$, $\Delta t_{EOG} = 6\text{d}$) was measured at a T_S of 18°C and a VWC of 0.42 while the lowest
 24 measured flux ($34 \mu\text{g N}_2\text{O-N m}^{-2} \text{ h}^{-1}$) on a similar Δt_{EOG} was measured at a low T_S (1°C) and a lower VWC (0.3). Maximum
 25 positive measured FB flux deviations (Sect. 2.7) from Eq. 3 were generally observed for wet ($VWC > 0.45$) and warm (>17
 26 $^\circ\text{C}$) soil conditions while low T_S and VWC resulted in negative flux deviations. Thus, the final regression model for urine
 27 patch emissions (Eq. 6) consists of multiple equations (Eq. 3, 7, 8) which relate the measured fluxes to the temporal decay
 28 (Eq. 3) and a deviation $\Delta F_{U,E}$ to it, where $\Delta F_{U,E}$ was parametrized as a function of environmental driving parameters T_S and
 29 VWC_U (Eq. 7 and 8, Fig. 9).

30

$$F_U = F_{U,temp} + \Delta F_{U,E} \quad (6)$$

31



$$\Delta F_{U,E} = (a_4 + b_4 \cdot VWC_U + c_4 \cdot T_S) \cdot Corr_{U,E}(\Delta t_{EOG}) \quad (7)$$

$Corr_{U,E}$ corrects $\Delta F_{U,E}$ for different urine patch ages as the deviation can be larger for relatively new patches compared to older ones. This correction factor was found to be a linear relationship ($p < 0.01$) between 1.35 for a Δt_{EOG} of 0 days (after the patch deposition) and 0.35 after 20 days. VWC_U (Eq. 8) accounts for different soil moisture conditions at the surface below an urine patch and nearby background areas and was parametrised as a function of VWC and Δt_{EOG} (Eq. 8).

$$VWC_U = VWC + a_5 \cdot \exp^{b_5 \cdot \Delta t_{EOG}} \quad (8)$$

3.3 Up-scaled chamber fluxes

3.3.1 Comparison between up-scaled chamber and EC fluxes

Generally the field scale fluxes represent the area integral of management related (excreta patches) and environmentally driven small scale fluxes. Therefore the relationships presented in Sect. 3.2.2 (dependency on excreta age) and Sect. 3.2.3 (environmental driving parameter) were applied to upscale the FB measurements to the paddock size during the GOP.

As shown exemplary for an 18-day period in Fig. 10b, the magnitude of the management related up-scaled paddock fluxes depended mainly on the grazing duration on the single paddocks (similar slope for different paddocks M11–M14). The maximum of the emissions was typically calculated at the end of the grazing period on the respective paddocks. The lower limit of the fluxes was given by the estimated background fluxes, especially at the beginning of a new rotation and stayed therefore rather constant for VWC values above 0.3 (Eq. 5, Sect. 3.2.3). Variations in environmental conditions (mainly important for soil moisture) led to rapid changes in the emission level as long as significant urine patch emissions were present. These rapid variations occurred typically after stronger precipitation events (as shown in Fig. 10a for onsite meteorological and soil measurements).

Upscaling the paddock fluxes to the EC footprint allowed a direct comparison with the EC fluxes on a half-hourly basis (Fig. 10c). The up-scaled FB fluxes compared well in magnitude with the measured EC fluxes and showed a comparable temporal behaviour. Nevertheless, the variations were less pronounced. While generally a response of the up scaled FB fluxes to variations of environmental driving parameter was observed, the response was rather limited in comparison to the measured EC fluxes.

Gapfilling of the EC fluxes (Sect. 2.5.3) allowed the calculation of the cumulative emissions during the GOP (solid lines in Fig. 11). Normalized per area, emission were very comparable between the two systems throughout the GOP and the seasonal sums of the emissions were in the order of $1500 \text{ g N}_2\text{O-N ha}^{-1}$. Cumulating the N_2O emissions not only enabled a more quantitative comparisons between the systems, but also allowed a better comparison between the two measurement approaches (Fig. 11). The emissions of the up-scaled FB matched the EC emissions rather well with differences of the



1 seasonal sums below 3 %. Distinct differences were mainly observed in May and June when FB derived emissions were
2 significantly overestimated compared to EC. At the end of the grazing period slightly lower emissions were estimated from
3 the upscaling routine compared to the measured EC emissions. Monthly absolute differences between the cumulative EC and
4 the up-scaled cumulative FB sums were normally distributed ($p < 0.05$) with 1σ values of 26 % and 25 % for system M and G,
5 respectively. Within this uncertainty range no difference between the two measurement approaches was observable.

6 **3.3.2 Emission breakdown into contribution sources**

7 The excellent match between the EC fluxes and the up-scaled chamber based fluxes showed that the used relationships with
8 excreta age and environmental drivers (see Sect. 3.2) was reasonable and allowed the separation into single emission sources
9 (Fig. 12). Except for the beginning of the grazing season when grazing rate was very low (see Fig. 2), the urine patch
10 emissions dominated the field scale fluxes. In May, this effect was even more pronounced due to the wet soil conditions.
11 Based on the upscaling, the averaged urine patch emission of both systems were responsible for about 57 % of the pasture
12 emissions. Background contributed to about 38 % and dung emissions to about 5 % to the overall field emissions. Both
13 systems had very similar contributions, with only 1 % difference in the dung contribution as a result of a different N
14 excretion ha^{-1} on the pasture by dung (Table 5). Background emissions were simulated to be constant for most of the GOP
15 due to the weak sensitivity of Eq. 5 to VWC and the undetected sensitivity towards soil temperature.

16 **4 Discussion**

17 **4.1 System related emissions**

18 The EC and up-scaled FB emission results presented in Sect. 3.3.1 were normalized by area and showed the emissions for
19 the EC footprint (see also summary in Table 5). The good agreement between the two independent approaches supports their
20 quality (incl. the upscaling procedure) in this study. The EC footprint is not necessarily fully representative for the whole
21 pasture system as the summed flux contributions of the central paddocks X.11, X.12 and X.21, X.22 already contributed
22 about 50 % to the measured EC flux during the GOP. Different grazing times on the individual paddocks, different soil
23 conditions or different crude protein contents in the grass (leading to different N in the excretion) might have influenced the
24 result. However we found no clear indication for differences between the rotation paddocks concerning their productivity or
25 other characteristics. Also an alternative up-scaling of the FB measurements to the entire pasture system (without taking the
26 EC footprint into account) representing the average emission over all rotation paddocks (Table 5, FB system emissions)
27 differed less than 4 % from the EC footprint related emissions.

28 The area related emissions discussed so far are not representative for assessing the mitigation effect of the N reduced diet
29 regarding N_2O emissions because the pasture system area also plays a major role. Taking into account the different pasture
30 sizes (1.88 ha vs. 2.51 ha for system M and G, see Table 5) needed for the different feeding strategies (Sect. 2.2) resulted in a
31 significant system difference of 960 ± 219 g $\text{N}_2\text{O-N}$. This corresponds to a reduction effect in N_2O emission of the N



1 optimised diet of about 25 % and demonstrates the ability of an N adjusted forage to reduce emissions. It also shows, that the
2 reduction effect was mainly triggered by the higher pasture area needed for a full grazing regime. The difference was based
3 only on the emissions of the system level and did not take into account e.g. the N₂O emissions related to the maize
4 production through fertilization.

5 **4.2 Grazing related emission factor**

6 Emissions as described in Sect. 4.1 enabled the comparison of the systems M and G and the discussion of the diet effects on
7 N₂O emission. However, values presented in literature or used in national inventories typically relate the found emissions to
8 the N input within a given time period. The annual grazing related EF (Table 5) was 1.24 ± 0.20 % for system M and $1.36 \pm$
9 0.26 % for system G. They are based on the cumulative emissions of the EC systems relative to the N excreted on the system
10 pastures during the GOP. Its uncertainty is defined by the combined uncertainty of the gap filling method (Sect. 3.3.1) and
11 the N input estimation (15 %). The difference in the EFs between the systems is therefore not statistically significant. The
12 resulting EF were smaller compared to the proposed default EF of IPCC guidelines for animal excreta (2%; IPCC, 2006) but
13 ranked towards the higher end compared to newer studies (0.59 % and 0.26 % for urine and dung patches combined from
14 cattle and sheep; Cai and Akiyama, 2016; 1.18 % and 0.31 % for cattle urine and dung; Krol et al., 2016). However, most of
15 these studies were performed on (manually applied) urine or dung patches only and thus important background contributions
16 might have been undetected. With the EC method, we measured the N₂O fluxes of the whole pasture, including background
17 areas which contributed significantly to the overall pasture emissions (Sect. 3.3.2) and thus lead to higher emissions
18 compared to studies looking only at the direct excreta effect. Hence, the EFs for excreta and retrieved by the EC method
19 cannot be compared directly, but the EC based EF by this study represents a possible maximum for the site and year.
20 Relating the up-scaled FB measurements to the N excretion estimates resulted in separated EFs of 1.13 ± 0.3 % and $0.17 \pm$
21 0.04 % for urine and dung, respectively (average of systems given due to small difference, Table 5), which supports the
22 suggestion of Krol et al. (2016) to disaggregate the EF by excreta type. The background emissions cannot be attributed to
23 one excreta type with high confidence, but the annual sum of $1.03 \text{ kg N}_2\text{O-N ha}^{-1} \text{ yr}^{-1}$ from this study (extrapolated, Eq. 5)
24 compares well with found background emissions by a meta study of Kim et al. (2013, median: 0.7 and mean $1.52 \text{ kg N}_2\text{O-N}$
25 $\text{ha}^{-1} \text{ yr}^{-1}$) for agricultural lands. In agricultural systems, these background emissions are often regarded as a late effect of
26 fertilization events in previous years (Bouwman, 1996; Gu et al., 2009). On pastures, trampling and grazing management can
27 also stimulate the N₂O production via denitrification due to soil compaction (Bhandral et al., 2007).

28 **4.3 Up-scaling of FB fluxes**

29 Urine patch emissions were parametrized with an exponential decay and maximum emissions of about $600 \mu\text{g N}_2\text{O-N m}^{-2} \text{ h}^{-1}$
30 that is close to the maximum averaged emissions measured by Barneze et al. (2015) from manually applied urine in
31 laboratory conditions and on a grassland. However, a large range of different emission dynamics and magnitudes from urine
32 patches are reported in literature (e.g. two emission peaks due to nitrification and denitrification; emission peak after a few



1 days with near exponential decay afterwards; significant emissions after weeks to month; Bell et al., 2015; Cardenas et al.,
2 2016; Chadwick et al., 2018b) with no clear trend. Nevertheless, a strong emission response to urine applications was usually
3 observed. Similar to our study, reported dung patch emissions by these studies were much lower compared to urine induced
4 emissions. The regressions relating the flux deviation (of urine patch emissions) to the soil parameters (Sect. 3.2.3) were
5 based on the northern soil profiles. The northern profile was already installed in 2013 and thus it was assumed that this
6 profile reports more reliable measurements. For up-scaling, only the soil measurements of the northern system were used for
7 consistency. Nevertheless, the soil measurements did not differ much between the two systems. As the field scale EC fluxes
8 and cumulative emissions were very similar for both systems as well, homogeneity on the pasture was assumed (as far as
9 concerned for up-scaling the FB measurements).

10 We found that pasture emissions were dominated by excreta emissions during the GOP (about 60 %). On a seasonal basis,
11 the up-scaled fluxes compared well with the gap filled EC measurements and justified the disaggregation of the up-scaled
12 field scale emissions. Especially during time periods where both FB fluxes and EC fluxes were measured (July – October)
13 the agreement between the systems was very good.

14 However, the retrieved regression resulted in a poor performance for certain soil conditions. The limited sensitivity towards
15 changes in *VWC* of the background fluxes is probably due to the fact that FB measurements were mainly performed during
16 dry soil conditions. Additionally, we have no certain explanation why we did not find a significant sensitivity of the
17 background fluxes towards changes in *T_s* as reported by other studies (Butterbach-Bahl et al., 2013; Schindlbacher, 2004).
18 Typically, increasing soil temperature lead to increased soil respiration which subsequently can lead to a depletion of soil
19 oxygen and further to higher denitrification rates. In contrast to background fluxes, fluxes of urine patches showed a clear
20 response to changes in *T_s* and *VWC*. Flux deviations from the temporal decrease could thus be parametrised with a double
21 linear regression (Sect. 3.2.3). This regression led to very high emissions from urine patches especially during wet soil
22 conditions and subsequently to a significant overestimation of the cumulative emissions in May and June compared to the
23 EC systems. *N₂O* emissions often have an emission optimum during moderately wet soil conditions (70-80 WFPS) while
24 completely anaerobic conditions can lead to a complete denitrification with only marginal *N₂O* emissions (Butterbach-Bahl
25 et al., 2013). A general trend towards lower emissions during very wet soil conditions was also observed by the EC systems
26 (not shown). However, in order to avoid mixing results of the different measurement systems and thus reducing the
27 explanatory power of the system inter-comparison we decided to base the environmental regression analysis (Sect. 3.2.3)
28 only on measured data by the FB.
29

30 **4.4 Advantages and problems of experimental setup**

31 The presented field campaign was designed to estimate the *N₂O* emissions of two parallel grazing systems and to compare
32 different feeding diets of the herds. Field scale emissions derived by the EC method resulted in a wide range of measured
33 emissions which were mainly driven by environmental and management related parameters. Nevertheless, the setup with two
34 towers allowed for a good comparison with a sufficient number of measured fluxes from both systems. Due to a delayed



1 installation of the EC tower at system G all fluxes prior mid of April had to be gap filled which resulted in a higher
2 associated uncertainty.

3 The excreted N modelled by the animal budget model at a temporal resolution of 1 day was needed in order to quantify the
4 EF of the two systems and to upscale FB chamber measurements to the field scale. Nevertheless, direct measurements would
5 have been preferable. However, as the N content in the excreta is highly variable (Betteridge et al., 2013) on a seasonal (e.g.
6 due to variability in the N content of the fodder) and short term scale (e.g. different urine volume, different cows, difference
7 between day and night) continuous measurements throughout the grazing period for a representative number of cows would
8 have been needed. This is only possible with measurement equipment directly placed on the cow. Beside the still
9 considerable uncertainty associated to these measurements they are often limited regarding animal welfare and not well
10 established (Misselbrook et al., 2016). Thus, they were not used in this study.

11 The combined approach of EC and FB measurements allowed the quantification of the uncertainty of the up-scaling routine
12 and the good match between the two measurement approaches justified the disaggregation of the different emission sources
13 on the pasture. The uncertainty associated to this up-scaling resulted mainly from missing FB measurements during wet soil
14 conditions (e.g. in spring) which prohibited the calculation of a more complex environmentally driven background and urine
15 emission regression. In summary, the experiment resulted in robust field scale emissions, enabled us to compare the two
16 systems and resulted in satisfying contribution estimates from the different emission sources.

17 **5 Concluding remarks**

18 The temporal dynamics of background areas and excreta patches were observed by fast-box (FB) chamber measurements on
19 the pasture. We found no significant temporal pattern of the background fluxes. Urine patch emissions were parametrised by
20 an exponential decay with time whereas a less pronounced dependency on excreta age of dung emissions was observed. This
21 relation was parametrised with a quadratic function and a maximum after about 10 days. On a field scale level, urine patch
22 emissions dominated the pasture emissions during the grazing season. Nevertheless, background fluxes contributed
23 significantly to the pasture emissions as well. The origin of these background fluxes is still uncertain and should be
24 addressed in further studies.

25 Taking the different size of the pastures into account, the emissions showed a clear difference of about 25 % between the two
26 systems and revealed the large potential of an N optimised feeding strategy to reduce N₂O emissions. The grazing related
27 EFs retrieved by the eddy covariance (EC) method were 1.24 ± 0.20 % for system M and 1.36 ± 0.26 % for system G and
28 were thus lower compared to the current default EF of 2 % provided by the guidelines of the IPCC. The combined approach
29 with EC and FB measurements proved to be appropriate to observe and quantify the magnitude of the pasture emissions and
30 the contribution of the single emission sources. The combined findings suggest the disaggregation of the excreta EF in single
31 EFs for urine and dung (1.13 ± 0.3 % and 0.17 ± 0.04 %, respectively).

32



1 *Data availability.* Data obtained in this study will be online available at the time of publication from the data repository
2 zenodo.org. (the DOI will be included in the final paper version).

3
4 *Competing interests.* The authors declare that they have no conflict of interest.

5
6 *Acknowledgements.*
7 We gratefully acknowledge the funding from the Swiss National Science Foundation (Project NICEGRAS, no. 155964) and
8 from the Swiss Federal Office for the Environment (Contract no. 16.0030.KP/P031-1675). We wish to thank Lukas
9 Eggerschwiler, Robin Giger, Walter Glauser, Andreas Mürger and Jens Leifeld for support in the field and helpful
10 discussions. We especially acknowledge the contribution of Harald Menzi in the design and planning of the experiment and
11 Arjan Hensen for lending the Fast-Box and advise how to use it. We are grateful to Albrecht Neftel for the helpful
12 discussions and advise concerning the measurements. We thank Daniel Bretscher for the support with the N balance
13 computation of the cows and the discussions of these data. Karl Voglmeier was additionally supported by a MICMoR
14 Fellowship through KIT/IMK-IFU.

15 **References**

- 16 Aarons, S. R., Gourley, C. J. P., Powell, J. M. and Hannah, M. C.: Estimating nitrogen excretion and deposition by lactating
17 cows in grazed dairy systems, *Soil Res.*, 55(6), 489, doi:10.1071/SR17033, 2017.
- 18 Ammann, C., Brunner, A., Spirig, C. and Neftel, A.: Technical note: Water vapour concentration and flux measurements
19 with PTR-MS, *Atmos Chem Phys*, 9, 2006.
- 20 Ammann, C., Flechard, C. R., Leifeld, J., Neftel, A. and Fuhrer, J.: The carbon budget of newly established temperate
21 grassland depends on management intensity, *Agric. Ecosyst. Environ.*, 121(1–2), 5–20, doi:10.1016/j.agee.2006.12.002,
22 2007.
- 23 Arriaga, H., Salcedo, G., Calsamiglia, S. and Merino, P.: Effect of diet manipulation in dairy cow N balance and nitrogen
24 oxides emissions from grasslands in northern Spain, *Agric. Ecosyst. Environ.*, 135(1–2), 132–139,
25 doi:10.1016/j.agee.2009.09.007, 2010.
- 26 Barneze, A. S., Minet, E. P., Cerri, C. C. and Misselbrook, T.: The effect of nitrification inhibitors on nitrous oxide
27 emissions from cattle urine depositions to grassland under summer conditions in the UK, *Chemosphere*, 119, 122–129,
28 doi:10.1016/j.chemosphere.2014.06.002, 2015.
- 29 Bates, G., Quin, B. and Bishop, P.: Low-cost detection and treatment of fresh cow urine patches, in *Moving farm systems to*
30 *improved attenuation.* (Eds L.D. Currie and L.L Burkitt), vol. 28, p. 12, Palmerston North, New Zealand. [online] Available
31 from: <http://flrc.massey.ac.nz/workshops/15/paperlist15.htm>, 2015.



- 1 Bell, M. J., Rees, R. M., Cloy, J. M., Topp, C. F. E., Bagnall, A. and Chadwick, D. R.: Nitrous oxide emissions from cattle
2 excreta applied to a Scottish grassland: Effects of soil and climatic conditions and a nitrification inhibitor, *Sci. Total*
3 *Environ.*, 508, 343–353, doi:10.1016/j.scitotenv.2014.12.008, 2015.
- 4 Betteridge, K., Costall, D. A., Li, F. Y., Luo, D. and Ganesh, S.: Why we need to know what and where cows are urinating –
5 a urine sensor to improve nitrogen models, *Proc N. Z. Grassl. Assoc.*, 75, 119–124, 2013.
- 6 Bhandral, R., Saggar, S., Bolan, N. and Hedley, M.: Transformation of nitrogen and nitrous oxide emission from grassland
7 soils as affected by compaction, *Soil Tillage Res.*, 94(2), 482–492, doi:10.1016/j.still.2006.10.006, 2007.
- 8 Biermann, T., Babel, W., Ma, W., Chen, X., Thiem, E., Ma, Y. and Foken, T.: Turbulent flux observations and modelling
9 over a shallow lake and a wet grassland in the Nam Co basin, Tibetan Plateau, *Theor. Appl. Climatol.*, 116(1–2), 301–316,
10 doi:10.1007/s00704-013-0953-6, 2014.
- 11 Bouwman, A. F.: Direct emission of nitrous oxide from agricultural soils, *Nutr. Cycl. Agroecosystems*, 46(1), 53–70,
12 doi:10.1007/BF00210224, 1996.
- 13 Butterbach-Bahl, K., Baggs, E. M., Dannenmann, M., Kiese, R. and Zechmeister-Boltenstern, S.: Nitrous oxide emissions
14 from soils: how well do we understand the processes and their controls?, *Philos. Trans. R. Soc. B Biol. Sci.*, 368(1621),
15 20130122–20130122, doi:10.1098/rstb.2013.0122, 2013.
- 16 Cai, Y. and Akiyama, H.: Nitrogen loss factors of nitrogen trace gas emissions and leaching from excreta patches in
17 grassland ecosystems: A summary of available data, *Sci. Total Environ.*, 572, 185–195, doi:10.1016/j.scitotenv.2016.07.222,
18 2016.
- 19 Cardenas, L. M., Thorman, R., Ashlee, N., Butler, M., Chadwick, D., Chambers, B., Cuttle, S., Donovan, N., Kingston, H.
20 and Lane, S.: Quantifying annual N₂O emission fluxes from grazed grassland under a range of inorganic fertiliser nitrogen
21 inputs, *Agric. Ecosyst. Environ.*, 136(3–4), 218–226, doi:10.1016/j.agee.2009.12.006, 2010.
- 22 Cardenas, L. M., Misselbrook, T. M., Hodgson, C., Donovan, N., Gilhespy, S., Smith, K. A., Dhanoa, M. S. and Chadwick,
23 D.: Effect of the application of cattle urine with or without the nitrification inhibitor DCD, and dung on greenhouse gas
24 emissions from a UK grassland soil, *Agric. Ecosyst. Environ.*, 235, 229–241, doi:10.1016/j.agee.2016.10.025, 2016.
- 25 Chadwick, D. R., Cardenas, L. M., Dhanoa, M. S., Donovan, N., Misselbrook, T., Williams, J. R., Thorman, R. E.,
26 McGeough, K. L., Watson, C. J., Bell, M., Anthony, S. G. and Rees, R. M.: The contribution of cattle urine and dung to
27 nitrous oxide emissions: Quantification of country specific emission factors and implications for national inventories, *Sci.*
28 *Total Environ.*, 635, 607–617, doi:10.1016/j.scitotenv.2018.04.152, 2018a.
- 29 Chadwick, D. R., Cardenas, L. M., Dhanoa, M. S., Donovan, N., Misselbrook, T., Williams, J. R., Thorman, R. E.,
30 McGeough, K. L., Watson, C. J., Bell, M., Anthony, S. G. and Rees, R. M.: The contribution of cattle urine and dung to
31 nitrous oxide emissions: Quantification of country specific emission factors and implications for national inventories, *Sci.*
32 *Total Environ.*, 635, 607–617, doi:10.1016/j.scitotenv.2018.04.152, 2018b.
- 33 Cowan, N. J., Norman, P., Famulari, D., Levy, P. E., Reay, D. S. and Skiba, U. M.: Spatial variability and hotspots of soil
34 N₂O fluxes from intensively grazed grassland, *Biogeosciences*, 12(5), 1585–1596, doi:10.5194/bg-12-1585-2015, 2015.



- 1 Felber, R.: Bridging the gap between animal and ecosystem emissions: Performance of CH₄ and CO₂ eddy covariance
2 measurements over a grazed pasture, ETH Zurich., 2015.
- 3 Felber, R., M \ddot{u} nger, A., Neftel, A. and Ammann, C.: Eddy covariance methane flux measurements over a grazed pasture:
4 effect of cows as moving point sources, *Biogeosciences*, 12(12), 3925–3940, doi:10.5194/bg-12-3925-2015, 2015.
- 5 Flechard, C. R., Ambus, P., Skiba, U., Rees, R. M., Hensen, A., van Amstel, A., Dasselaar, A. van den P., Soussana, J.-F.,
6 Jones, M., Clifton-Brown, J., Raschi, A., Horvath, L., Neftel, A., Jocher, M., Ammann, C., Leifeld, J., Fuhrer, J., Calanca,
7 P., Thalman, E., Pilegaard, K., Di Marco, C., Campbell, C., Nemitz, E., Hargreaves, K. J., Levy, P. E., Ball, B. C., Jones, S.
8 K., van de Bulk, W. C. M., Groot, T., Blom, M., Domingues, R., Kasper, G., Allard, V., Ceschia, E., Cellier, P., Laville, P.,
9 Henault, C., Bizouard, F., Abdalla, M., Williams, M., Baronti, S., Berretti, F. and Grosz, B.: Effects of climate and
10 management intensity on nitrous oxide emissions in grassland systems across Europe, *Agric. Ecosyst. Environ.*, 121(1–2),
11 135–152, doi:10.1016/j.agee.2006.12.024, 2007.
- 12 Flesch, T. K. and Wilson, J. D.: Estimating Tracer Emissions with a Backward Lagrangian Stochastic Technique, in
13 *Agronomy Monograph*, edited by J. L. Hatfield and J. M. Baker, American Society of Agronomy, Crop Science Society of
14 America, and Soil Science Society of America., 2005.
- 15 Flesch, T. K., Wilson, J. D., Harper, L. A., Crenna, B. P. and Sharpe, R. R.: Deducing Ground-to-Air Emissions from
16 Observed Trace Gas Concentrations: A Field Trial, *J. Appl. Meteorol.*, 43(3), 487–502, doi:10.1175/1520-
17 0450(2004)043<0487:DGEFOT>2.0.CO;2, 2004.
- 18 Foken, T., Leuning, R., Oncley, S. R., Mauder, M. and Aubinet, M.: Corrections and Data Quality Control, in *Eddy*
19 *Covariance*, edited by M. Aubinet, T. Vesala, and D. Papale, pp. 85–131, Springer Netherlands, Dordrecht., 2012.
- 20 Fuchs, K., H \ddot{o} rtnagl, L., Buchmann, N., Eugster, W., Snow, V. and Merbold, L.: Management matters: Testing a mitigation
21 strategy for nitrous oxide emissions on intensively managed grassland, *Biogeosciences Discuss.*, 1–43, doi:10.5194/bg-2018-
22 192, 2018.
- 23 Gu, J., Zheng, X. and Zhang, W.: Background nitrous oxide emissions from croplands in China in the year 2000, *Plant Soil*,
24 320(1–2), 307–320, doi:10.1007/s11104-009-9896-1, 2009.
- 25 H \ddot{a} ni, C.: bLSmodelR – An atmospheric dispersion model in R. [online] Available from: [http://www.agrammon.ch/
26 documents-to-download/blsmodelr/](http://www.agrammon.ch/documents-to-download/blsmodelr/) (Accessed 24 October 2017), 2017.
- 27 H \ddot{a} ni, C., Flechard, C., Neftel, A., Sintermann, J. and Kupper, T.: Accounting for Field-Scale Dry Deposition in Backward
28 Lagrangian Stochastic Dispersion Modelling of NH₃ Emissions, , doi:10.20944/preprints201803.0026.v1, 2018.
- 29 Hensen, A., Groot, T. T., van den Bulk, W. C. M., Vermeulen, A. T., Olesen, J. E. and Schelde, K.: Dairy farm CH₄ and
30 N₂O emissions, from one square metre to the full farm scale, *Agric. Ecosyst. Environ.*, 112(2–3), 146–152,
31 doi:10.1016/j.agee.2005.08.014, 2006.
- 32 IPCC: 2006 IPCC Guidelines for National Greenhouse Gas Inventories, Prepared by the National Greenhouse Gas
33 Inventories Programme, Eggleston H.S., Buendia L., Miwa K., Ngara T. and Tanabe K. (eds). Published: IGES, Japan.,
34 2006.



- 1 Jones, S. K., Famulari, D., Di Marco, C. F., Nemitz, E., Skiba, U. M., Rees, R. M. and Sutton, M. A.: Nitrous oxide
2 emissions from managed grassland: a comparison of eddy covariance and static chamber measurements, *Atmospheric Meas.*
3 *Tech.*, 4(10), 2179–2194, doi:10.5194/amt-4-2179-2011, 2011.
- 4 Kaimal, J. C. and Finnigan, J. J.: *Atmospheric boundary layer flows: their structure and measurement*, Oxford University
5 Press, New York., 1994.
- 6 Kim, D.-G., Giltrap, D. and Hernandez-Ramirez, G.: Background nitrous oxide emissions in agricultural and natural lands: a
7 meta-analysis, *Plant Soil*, 373(1–2), 17–30, doi:10.1007/s11104-013-1762-5, 2013.
- 8 Krol, D. J., Carolan, R., Minet, E., McGeough, K. L., Watson, C. J., Forrester, P. J., Lanigan, G. J. and Richards, K. G.:
9 Improving and disaggregating N₂O emission factors for ruminant excreta on temperate pasture soils, *Sci. Total Environ.*,
10 568, 327–338, doi:10.1016/j.scitotenv.2016.06.016, 2016.
- 11 Langford, B., Acton, W., Ammann, C., Valach, A. and Nemitz, E.: Eddy-covariance data with low signal-to-noise ratio:
12 time-lag determination, uncertainties and limit of detection, *Atmospheric Meas. Tech.*, 8(10), 4197–4213, doi:10.5194/amt-
13 8-4197-2015, 2015.
- 14 Luo, J., Wyatt, J., van der Weerden, T. J., Thomas, S. M., de Klein, C. A. M., Li, Y., Rollo, M., Lindsey, S., Ledgard, S. F.,
15 Li, J., Ding, W., Qin, S., Zhang, N., Bolan, N., Kirkham, M. B., Bai, Z., Ma, L., Zhang, X., Wang, H., Liu, H. and Rys, G.:
16 Potential Hotspot Areas of Nitrous Oxide Emissions From Grazed Pastoral Dairy Farm Systems, in *Advances in Agronomy*,
17 vol. 145, pp. 205–268, Elsevier., 2017.
- 18 MeteoSwiss: Climate normals Fribourg/Posieux, [online] Available from:
19 [www.meteoschweiz.admin.ch/product/output/climate-data/climate-diagrams-normal-values-station-](http://www.meteoschweiz.admin.ch/product/output/climate-data/climate-diagrams-normal-values-station-processing/GRA/climsheet_GRA_np8110_e.pdf)
20 [processing/GRA/climsheet_GRA_np8110_e.pdf](http://www.meteoschweiz.admin.ch/product/output/climate-data/climate-diagrams-normal-values-station-processing/GRA/climsheet_GRA_np8110_e.pdf) (Accessed 31 January 2018), 2018.
- 21 Mishurov, M. and Kiely, G.: Gap-filling techniques for the annual sums of nitrous oxide fluxes, *Agric. For. Meteorol.*,
22 151(12), 1763–1767, doi:10.1016/j.agrformet.2011.07.014, 2011.
- 23 Misselbrook, T., Fleming, H., Camp, V., Umstatter, C., Duthie, C.-A., Nicoll, L. and Waterhouse, T.: Automated monitoring
24 of urination events from grazing cattle, *Agric. Ecosyst. Environ.*, 230, 191–198, doi:10.1016/j.agee.2016.06.006, 2016.
- 25 Orr, R. J., Griffith, B. A., Champion, R. A. and Cook, J. E.: Defaecation and urination behaviour in beef cattle grazing semi-
26 natural grassland, *Appl. Anim. Behav. Sci.*, 139(1–2), 18–25, doi:10.1016/j.applanim.2012.03.013, 2012.
- 27 Oudshoorn, F. W., Kristensen, T. and Nadimi, E. S.: Dairy cow defecation and urination frequency and spatial distribution in
28 relation to time-limited grazing, *Livest. Sci.*, 113(1), 62–73, doi:10.1016/j.livsci.2007.02.021, 2008.
- 29 Papale, D.: Data Gap Filling, in *Eddy Covariance*, edited by M. Aubinet and T. Vesala, pp. 159–172, Springer Netherlands,
30 Dordrecht., 2012.
- 31 Pedersen, A. R., Petersen, S. O. and Schelde, K.: A comprehensive approach to soil-atmosphere trace-gas flux estimation
32 with static chambers, *Eur. J. Soil Sci.*, 61(6), 888–902, doi:10.1111/j.1365-2389.2010.01291.x, 2010.
- 33 Portmann, R. W., Daniel, J. S. and Ravishankara, A. R.: Stratospheric ozone depletion due to nitrous oxide: influences of
34 other gases, *Philos. Trans. R. Soc. B Biol. Sci.*, 367(1593), 1256–1264, doi:10.1098/rstb.2011.0377, 2012.



- 1 R Core Team: R: A Language and Environment for Statistical Computing, R Foundation for Statistical Computing, Vienna,
2 Austria. [online] Available from: <https://www.R-project.org/>, 2016.
- 3 Reay, D. S., Davidson, E. A., Smith, K. A., Smith, P., Melillo, J. M., Dentener, F. and Crutzen, P. J.: Global agriculture and
4 nitrous oxide emissions, *Nat. Clim. Change*, 2(6), 410–416, doi:10.1038/nclimate1458, 2012.
- 5 Sagar, S., Giltrap, D. L., Davison, R., Gibson, R., de Klein, C. A., Rollo, M., Ettema, P. and Rys, G.: Estimating direct N₂O
6 emissions from sheep, beef, and deer grazed pastures in New Zealand hill country: accounting for the effect of land slope on
7 the N₂O emission factors from urine and dung, *Agric. Ecosyst. Environ.*, 205, 70–78, doi:10.1016/j.agee.2015.03.005, 2015.
- 8 Schindlbacher, A.: Effects of soil moisture and temperature on NO, NO₂, and N₂O emissions from European forest soils,
9 *J. Geophys. Res.*, 109(D17), doi:10.1029/2004JD004590, 2004.
- 10 Schmid, H. P.: Footprint modeling for vegetation atmosphere exchange studies: a review and perspective, *Agric. For.
11 Meteorol.*, 113(1–4), 159–183, doi:10.1016/S0168-1923(02)00107-7, 2002.
- 12 Selbie, D. R., Buckthought, L. E. and Shepherd, M. A.: The Challenge of the Urine Patch for Managing Nitrogen in Grazed
13 Pasture Systems, in *Advances in Agronomy*, vol. 129, pp. 229–292, Elsevier., 2015.
- 14 Villettaz Robichaud, M., de Passillé, A. M., Pellerin, D. and Rushen, J.: When and where do dairy cows defecate and
15 urinate?, *J. Dairy Sci.*, 94(10), 4889–4896, doi:10.3168/jds.2010-4028, 2011.
- 16 Voglmeier, K., Jocher, M., Häni, C. and Ammann, C.: Ammonia emission measurements of an intensively grazed pasture -
17 Discussion, *Biogeosciences Discuss.*, 1–32, doi:10.5194/bg-2018-86, 2018.
- 18 Wilson, J. D., Flesch, T. K. and Crenna, B. P.: Estimating Surface-Air Gas Fluxes by Inverse Dispersion Using a Backward
19 Lagrangian Stochastic Trajectory Model, in *Geophysical Monograph Series*, edited by J. Lin, D. Brunner, C. Gerbig, A.
20 Stohl, A. Luhar, and P. Webley, pp. 149–162, American Geophysical Union, Washington, D. C., 2013.
- 21 Yan, T., Frost, J. P., Agnew, R. E., Binnie, R. C. and Mayne, C. S.: Relationships among manure nitrogen output and dietary
22 and animal factors in lactating dairy cows, *J. Dairy Sci.*, 89(10), 3981–3991, 2006.
- 23 Zhao, X. and Huang, Y.: A Comparison of Three Gap Filling Techniques for Eddy Covariance Net Carbon Fluxes in Short
24 Vegetation Ecosystems, *Adv. Meteorol.*, 2015, 1–12, doi:10.1155/2015/260580, 2015.

25
26
27
28
29
30
31
32



1 **Table 1: Soil parameters measured at different depth and averaged over four locations on the pasture. The measurements are**
 2 **given as mean \pm 1 standard deviation.**

Parameter	Surface Layer	Soil layer
Depth (cm)	5-10	25-30
Pore volume (%)	57 \pm 4	47 \pm 2
Bulk density (g cm ⁻³)	1.09 \pm 0.11	1.37 \pm 0.06
pH (-)	6.0 \pm 0.3	6.2 \pm 0.4
Sand (%)	42.6 \pm 2.5	45.6 \pm 3.2
Clay (%)	18.7 \pm 1.7	18.1 \pm 2.0
Silt (%)	33.0 \pm 1.3	34.2 \pm 1.6
Humus (%)	5.7 \pm 0.3	2.1 \pm 0.1
Depth (cm)	0-10	10-20
Total N (%)	0.38 \pm 0.03	0.27 \pm 0.04
Total C (%)	3.76 \pm 0.20	2.49 \pm 0.43
C:N (-)	9.9 \pm 0.2	9.2 \pm 0.5
Depth (cm)	0-5	5-15
NH ₄ ⁺ (mg kg ⁻¹)	5.0 \pm 3.1	2.8 \pm 1.6
NO ₃ ⁻ (mg kg ⁻¹)	17.2 \pm 8.8	9.2 \pm 5.1

3

4

5

6

7

8

9

10

11

12

13

14



1 **Table 2: Measured averages ± standard deviation of observed cow properties, feed protein contents, and resulting urine N and**
 2 **faeces N of the Swiss dairy cow nitrogen budget model for both pasture systems during the grazing season 2016.**

Input parameter (units)	System M	System G
Number of cows	12	12
Milk yield, ECM (kg cow ⁻¹ day ⁻¹)	25.1±2.9	24.2±3.7
Animal weight (kg)	633±14	633±10
Grass crude protein (g kg-DM ⁻¹)	195±23	196±23
Maize crude protein (g kg-DM ⁻¹)	84±8	n.a.
Urine N (g cow ⁻¹ d ⁻¹)	250±54	314±71
Dung N (g cow ⁻¹ d ⁻¹)	154±9	155±12

3
4
5
6
7
8
9
10
11
12
13
14
15
16
17
18
19
20
21
22
23
24
25
26



1 **Table 3: Flux measurements (mean ± std) of background and excreta patches averaged over 20 days following a new rotation.**

Measurement location	System M	System G
Background ($\mu\text{g N}_2\text{O-N m}^{-2} \text{ h}^{-1}$)	8 ± 8	5 ± 8
Urine ($\mu\text{g N}_2\text{O-N m}^{-2} \text{ h}^{-1}$)	121 ± 130	162 ± 190
Dung ($\mu\text{g N}_2\text{O-N m}^{-2} \text{ h}^{-1}$)	16 ± 18	35 ± 60

2

3

4

5

6

7

8

9

10

11

12

13

14

15

16

17

18

19

20

21

22

23

24

25

26

27

28



1 **Table 4: Coefficients (a-c), corresponding indices i and significance levels for the different equations presented in Sect. 3.2.**

Equation	i	a_i	b_i	c_i
Eq. 3	1	5.9E-4 ***	-8.2E-2 **	
Eq. 4	2	2.3E-5 *	4.8E-6 *	-2.5E-7 *
Eq. 5	3	1.26E-5 ***	2.67E-1 ***	1.22E-2 *
Eq. 7	4	-1.49E-3 ***	2.90E-3 ***	2.39E-5 **
Eq. 8	5	9.8E-2 ***	-8.6E-2 **	

2 ***Significant at level $p < 0.001$; **Significant at level $p < 0.01$; *Significant at level $p < 0.05$

3
4
5
6
7
8
9
10
11
12
13
14
15
16
17
18
19
20
21
22
23
24
25
26
27
28



1 **Table 5: Summary of grazing emission results for both pasture systems. The table shows the emissions normalized per area (first**
 2 **part), the area integrated emissions (second part), the EF (third part) and the disaggregation of pasture emissions into single**
 3 **emission sources (forth part). The uncertainties are given as 1σ .**

Parameter	System M	System G
EC emission (kg N ₂ O-N ha ⁻¹)	1.49 ± 0.21	1.49 ± 0.27
FB emissions up-scaled to EC footprint (kg N ₂ O-N ha ⁻¹)	1.51 ± 0.39	1.50 ± 0.37
FB emissions up-scaled to system (kg N ₂ O-N ha ⁻¹)	1.48 ± 0.38	1.48 ± 0.37
Pasture system area (ha)	1.88	2.51
EC integral system emission EC (kg N ₂ O-N)	2.79 ± 0.39	3.75 ± 0.68
N input total (kg ha ⁻¹)	120 ± 9	110 ± 8
N input urine (kg ha ⁻¹)	74 ± 6	73 ± 6
EF total (%)	1.24 ± 0.20	1.36 ± 0.26
EF urine (%)	1.12 ± 0.30	1.15 ± 0.30
EF dung (%)	0.16 ± 0.04	0.17 ± 0.04
FB urine emission up-scaled to system (kg N ₂ O-N ha ⁻¹)	0.83 ± 0.22	0.84 ± 0.21
FB dung emission up-scaled to system FAD-FB (kg N ₂ O-N ha ⁻¹)	0.08 ± 0.02	0.06 ± 0.02

4

5

6

7

8

9

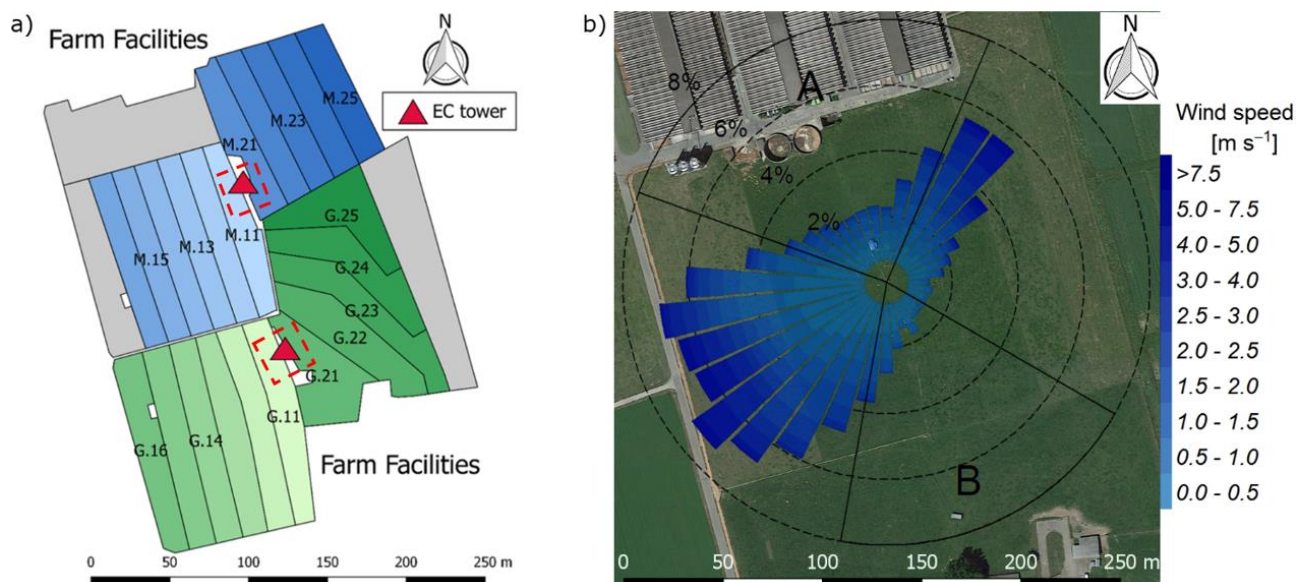
10

11

12

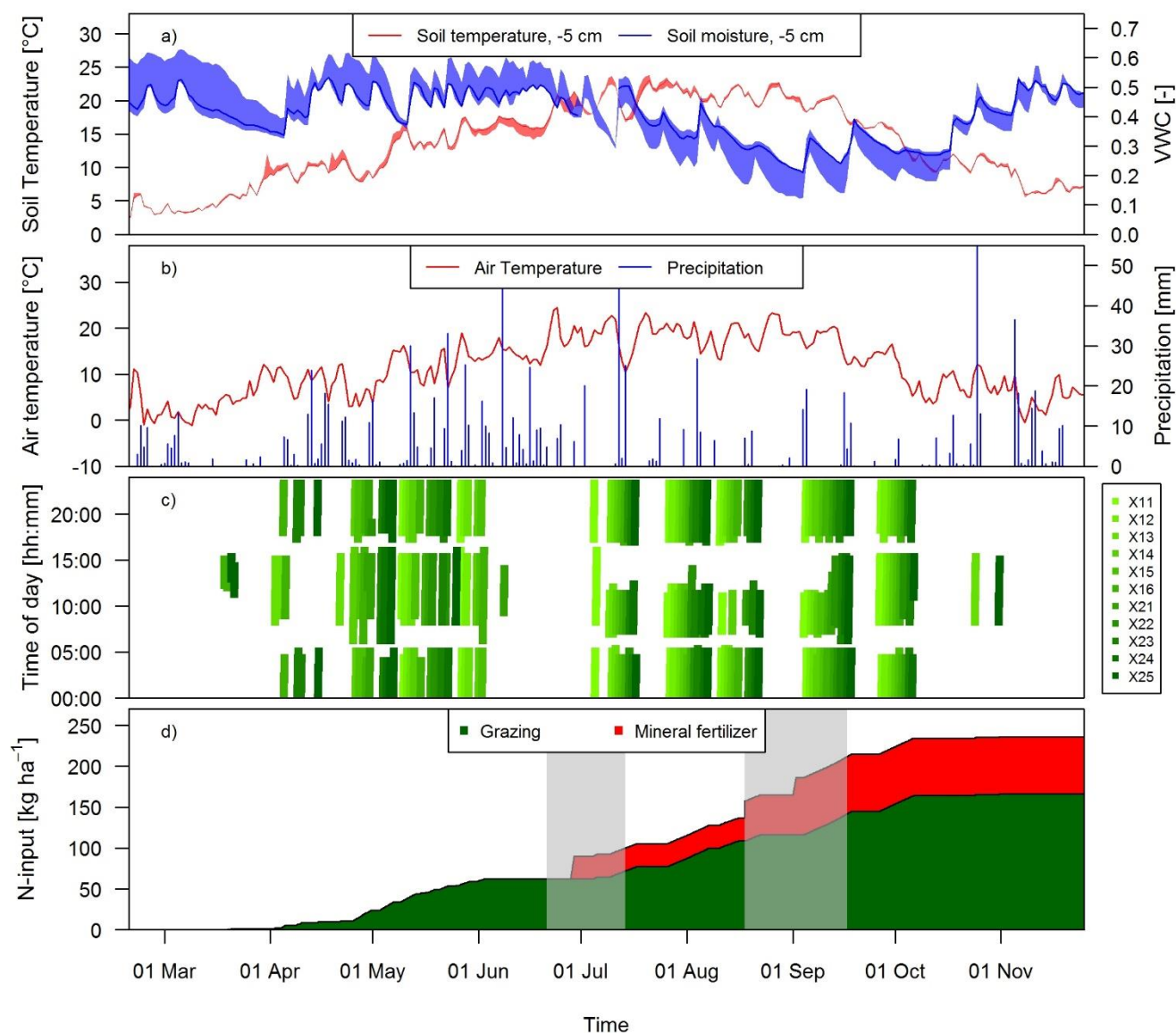
13

14



1
2 **Figure 1: a):** Measurement site with the pastures for the two herds (blue: grass diet with additional maize silage; green: full
3 **grazing regime; grey: optional pasture areas) and the division into the paddocks (M.11–M.31, G.11–G.31). Additionally the**
4 **location of the two EC towers and the area of the chamber measurements (red dashed rectangles) are shown. b) Wind distribution**
5 **for the northern sonic anemometer with the corresponding sector contributions (black dotted circles) for the period May –**
6 **October 2016. The areas A and B indicate wind sectors from which advection from nearby farm building can occur. The wind**
7 **distribution was overlaid on a Google Earth image of the experimental area (Map data: Google, DigitalGlobe)**

8
9
10

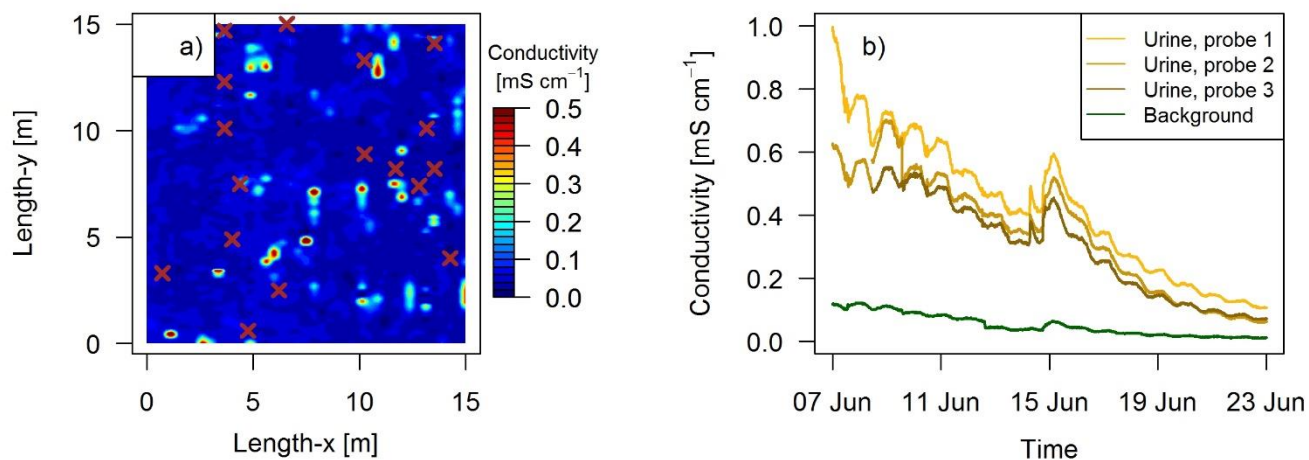


1

2 **Figure 2: Time series of a) daily averaged soil temperature and moisture at a depth of 5 cm measured at system M (solid lines) and**
 3 **spread of the four measurement locations, b) daily air temperature at 2 m above ground and precipitation at the measurement**
 4 **site, c) grazing duration on the single paddocks of the pasture (X: both pasture systems M and G) for the study year 2016 and d) N**
 5 **input to system M shortly before and during the main grazing season in 2016. Fertilizer was applied two times. The second**
 6 **application in August was split in two parts due to a delayed fertilization on the eastern part of the pasture (X.21-X.25). The grey**
 7 **shaded areas indicate special time periods influenced by fertilization or harvest events as explained in more detail in Sect. 2.5.2.**

8

9



1

2 **Figure 3: a) Measured conductivity within a quadratic 15 x 15 m intensive observation area on the 3rd of October, 2016 in paddock**
 3 **X.11. High values ($>0.15 \text{ mS cm}^{-1}$) indicate urine patch locations and brown crosses indicate observed dung pats. b) Conductivity**
 4 **measured continuously during a field experiment in 2017 with four GS3 sensors.**

5

6

7

8

9

10

11

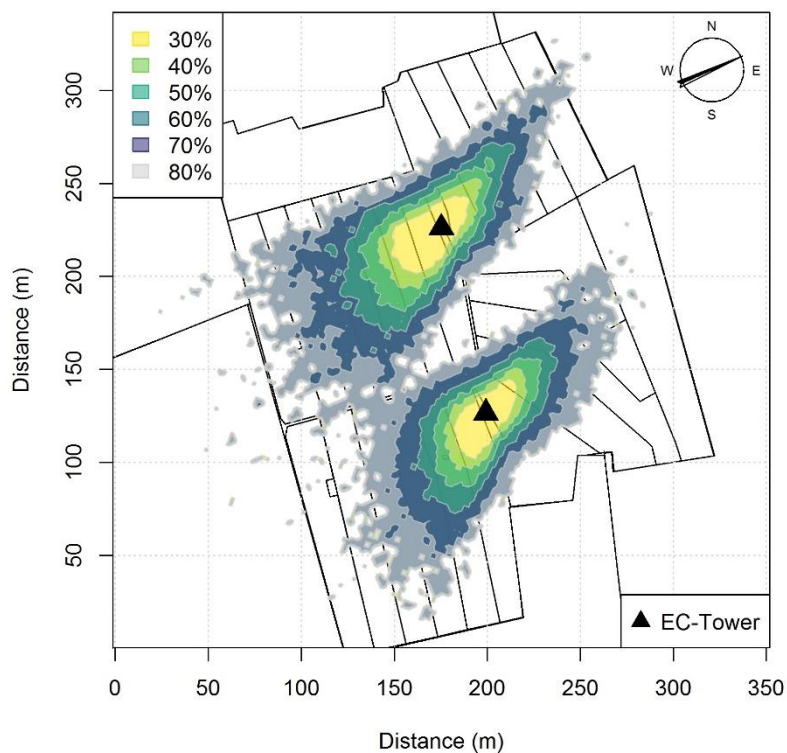
12

13

14

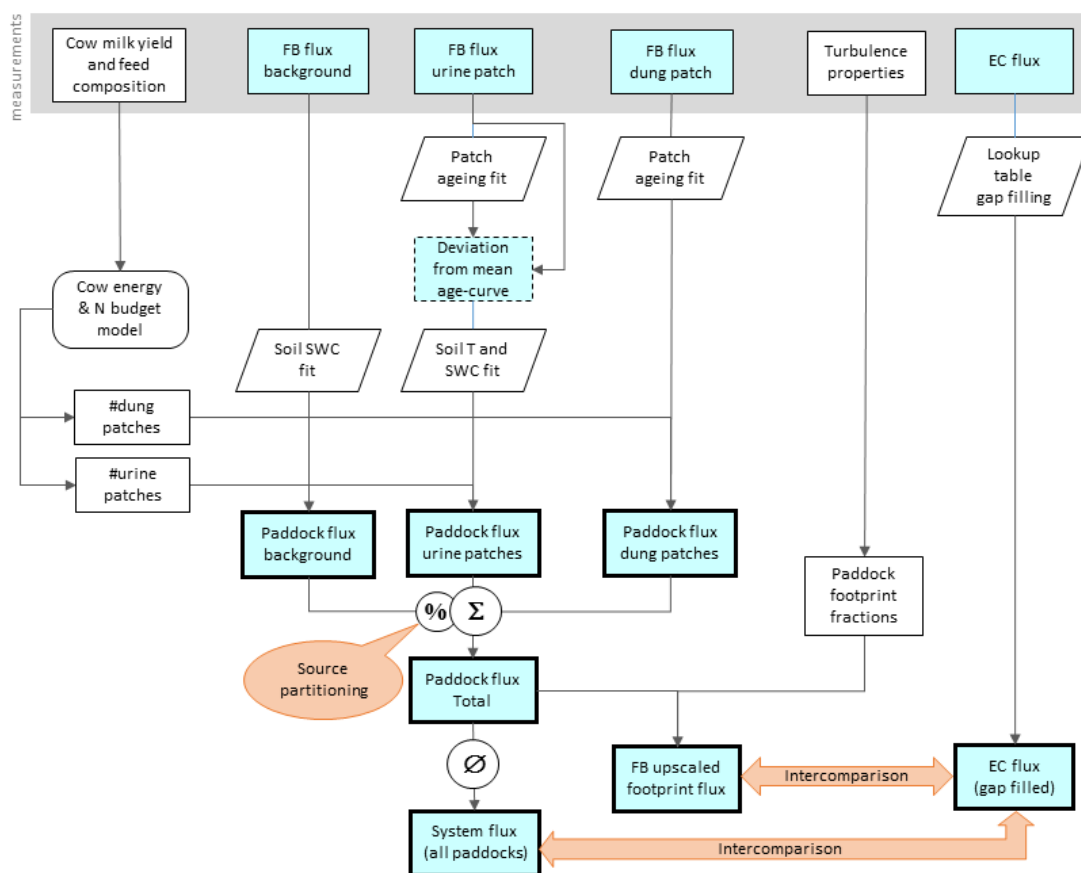
15

16



1
2
3
4
5
6

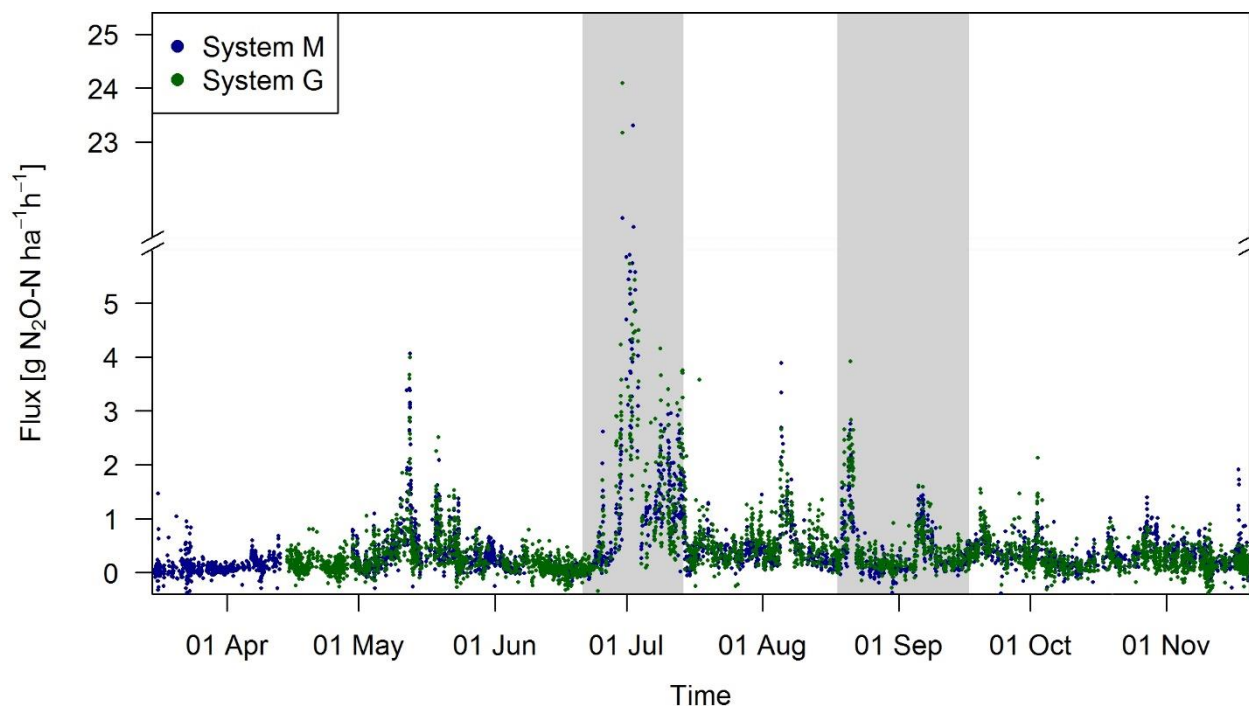
Figure 4: Footprint climatology for both EC towers averaged for the time period between 15th March 2016 and 15th November 2016. The legend values indicate the percentage of the total footprint weight.



1

2 **Figure 5: Flowchart of upscaling procedure to compare small scale chamber fluxes with EC fluxes and to estimate the contribution**
 3 **of excreta emissions to the overall pasture emission. Rectangular shapes indicate data sets / time series data. Time series data with**
 4 **thin frames have gaps whereas bold frames indicate complete data sets. The light blue colour specifies N₂O flux data. Other**
 5 **shapes show operations (e.g. fit or gap-filling routines).**

6



1

2 **Figure 6: Time series of half-hourly EC flux measurements in both systems during the grazing season. The grey shaded areas**
3 **indicate the time periods which were influenced by fertilization events or harvest and which were excluded from further analysis.**
4 **One value (28.7 g N₂O-N ha⁻¹ h⁻¹ on system M) was skipped for better readability.**

5

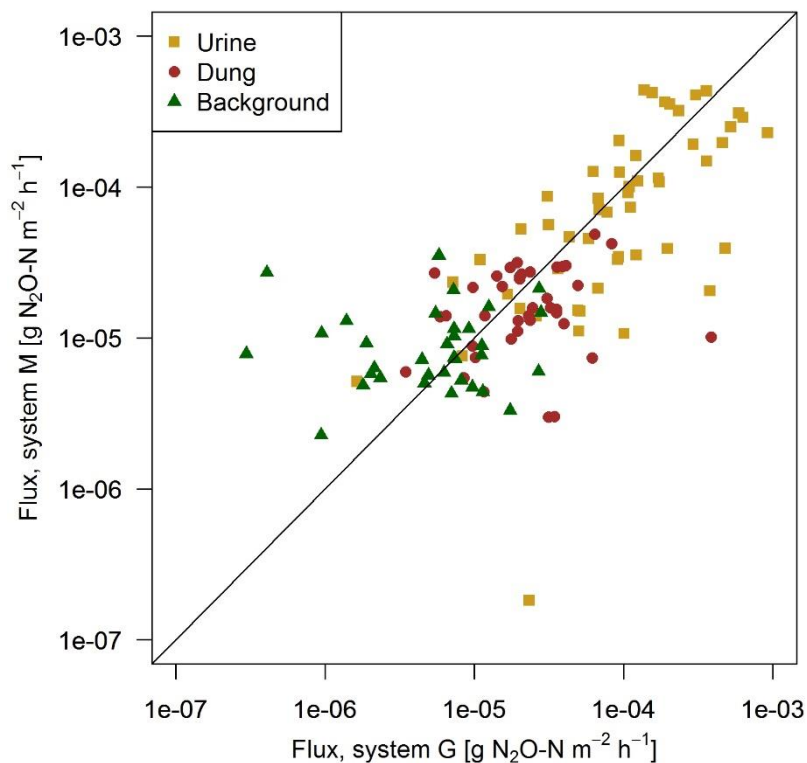
6

7

8

9

10



1

2 **Figure 7: Scatterplot shows the comparison of fluxes with similar excreta ages between system M and system G. The black line**
3 **indicates the 1:1 line.**

4

5

6

7

8

9

10

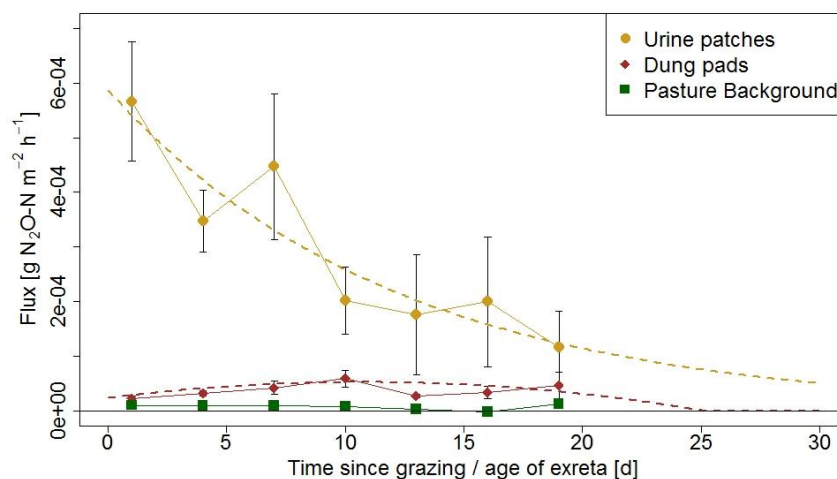
11

12

13

14

15



1

2 **Figure 8: N₂O Flux evolution with time for urine patches, dung pats and background areas. The fluxes were averaged over 3-day**
3 **periods and the error bars show the standard error of the measurements. The dotted lines show the fitted curves through the**
4 **averaged values of urine and dung patches.**

5

6

7

8

9

10

11

12

13

14

15

16

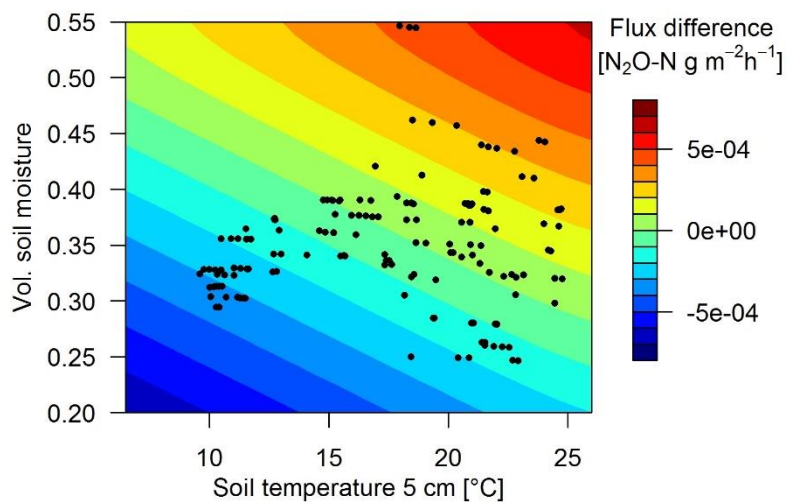
17

18

19

20

21



1

2 **Figure 9:** Surface plot shows the estimated N₂O flux deviation (Eq. 6, 7; $Corr_{U,E} = 0$) from the exponential fit (Eq. 3) for urine
3 patches depending on soil moisture VWC_U and temperature at a depth of 5 cm. The black dots indicate the conditions under which
4 flux measurements were obtained.

5

6

7

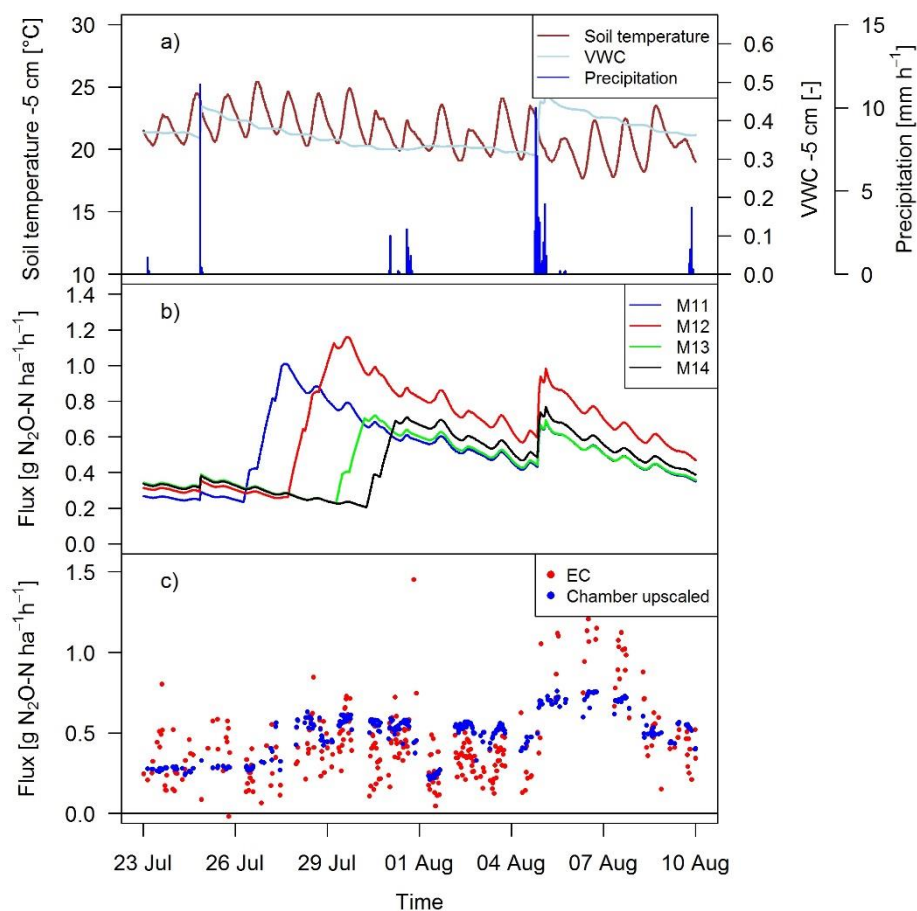
8

9

10

11

12



1

2 **Figure 10: Time series of a) environmental parameters and b) up-scaled FB fluxes (Sect. 2.7) for different paddocks on system M.**
 3 **c) EC and up-scaled footprint-weighted FB N₂O fluxes during a full rotation between 23th September and 10th August for system**
 4 **M.**

5

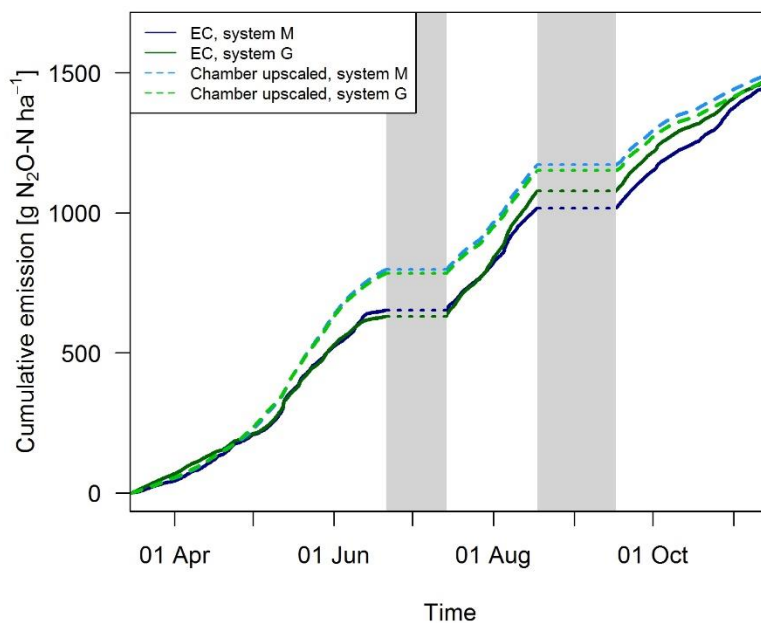
6

7

8

9

10



1

2 **Figure 11: a) Cumulative emissions for both systems obtained with FB and EC technique during GOP. The grey shaded bars**
3 **indicate time periods which were excluded due to significant overlapping N₂O emissions from fertilization / harvest and grazing**
4 **(Sect. 2.5, 3.1).**

5

6

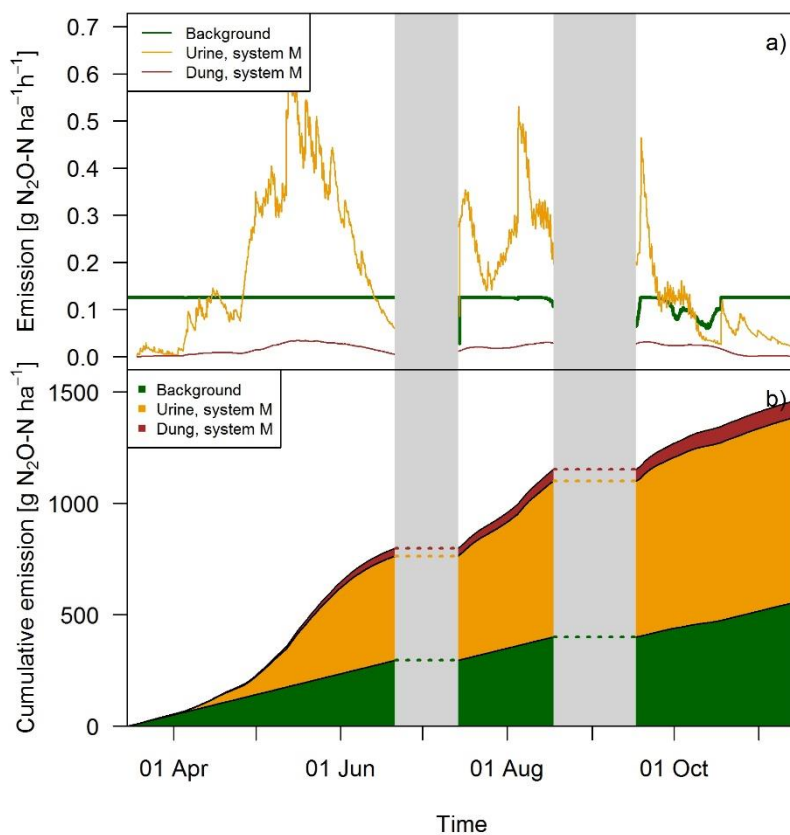
7

8

9

10

11



1

2 **Figure 12: a) Time series of paddock-averaged up-scaled FB fluxes for all three emission sources for system M during the grazing**
3 **season and b) retrieved cumulative emission contribution of these emission sources to the overall field emission.**